



## **Investigation of Permeable Aquifers at the Contact Zones of Basaltic Lava Flow**

Thesis of 60 ECTS credits submitted to the School of Science and Engineering  
at Reykjavík University in partial fulfillment of  
the requirements for the degree of  
**Master of Science (M.Sc.) in Sustainable Energy  
Science**

June 2024

Supervisors:

Juliet Ann Newson, Supervisor  
Professor, Reykjavík University, Iceland

Examiner:

Mike O'Sullivan, Examiner  
Professor, Auckland University, New Zealand



Copyright

Yonathan Hary Hutagalung

June 2024



# **Investigation of Permeable Aquifers at the Contact Zones of Basaltic Lava Flow**

Yonathan Hary Hutagalung

June 2024

## **Abstract**

The research is the first step in an investigation into various geometries of permeable zone that exist at contact between basaltic lava flows using numerical simulator AUTOUGH2. The study developed the modelling workflow and the scripts required to generate the models and plot the result graphically. The model development started with a radial model, proceeds to a two-dimensional rectangular model where the output is compared to the radial model to validate whether it provides a reasonable result. Furthermore, three dimensional models which modelled both as porous medium and fractured rock using MINC module in TOUGH2 were constructed where the permeable aquifer enclosed in between less permeable rocks. The geometry of the permeable layer is different in each model. The actual geometry of the aquifer has been designed as a regular grid of mountains and valleys where the peak height and distance between peaks differ for each model. Initially, drone mapping was intended to map exposed and relatively fresh lava surface (recent to **approximately as old as 13 to 14 million years old**) for data on possible forms of these contact aquifers. However, due to harsh winter conditions these have been covered by snow and/or wind has been excessively strong for the duration of the project. Hence, the aquifer geometry was generated using TIM, which is pre- and post- processor for TOUGH2.

The response to injection from one central well for these models shows that it is possible to see the effects of permeable layer geometry. It appears that the geometry of the aquifer influences the injection pressure, in that greater amplitude and shorter wavelength is related to decrease in injection pressure. However, one caveat is that the overall volume of the permeable layer was also increased. This was unavoidable due to the coarseness of the model grid and future work needs to take this into account. In addition, more fieldwork required to produce more realistic representation of the possible geometry of the buried lava surfaces that form these permeable aquifers.



# Titl verkefnis

Yonathan Hary Hutagalung

júní 2024

## Útdráttur

Lorem ipsum dolor sit amet, consectetur adipiscing elit. Ut purus elit, vestibulum ut, placerat ac, adipiscing vitae, felis. Curabitur dictum gravida mauris. Nam arcu libero, nonummy eget, consectetur id, vulputate a, magna. Donec vehicula augue eu neque. Pellentesque habitant morbi tristique senectus et netus et malesuada fames ac turpis egestas. Mauris ut leo. Cras viverra metus rhoncus sem. Nulla et lectus vestibulum urna fringilla ultrices. Phasellus eu tellus sit amet tortor gravida placerat. Integer sapien est, iaculis in, pretium quis, viverra ac, nunc. Praesent eget sem vel leo ultrices bibendum. Aenean faucibus. Morbi dolor nulla, malesuada eu, pulvinar at, mollis ac, nulla. Curabitur auctor semper nulla. Donec varius orci eget risus. Duis nibh mi, congue eu, accumsan eleifend, sagittis quis, diam. Duis eget orci sit amet orci dignissim rutrum.



# **Investigation of Permeable Aquifers at the Contact Zones of Basaltic Lava Flow**

Yonathan Hary Hutagalung

Thesis of 60 ECTS credits submitted to the School of Science and Engineering  
at Reykjavík University in partial fulfillment of  
the requirements for the degree of  
**Master of Science (M.Sc.) in Sustainable Energy Science**

June 2024

Student:

---

Yonathan Hary Hutagalung

Supervisors:

---

Juliet Ann Newson

Examiner:

---

Michael O'Sullivan



The undersigned hereby grants permission to the Reykjavík University Library to reproduce single copies of this Thesis entitled **Investigation of Permeable Aquifers at the Contact Zones of Basaltic Lava Flow** and to lend or sell such copies for private, scholarly or scientific research purposes only.

The author reserves all other publication and other rights in association with the copyright in the Thesis, and except as herein before provided, neither the Thesis nor any substantial portion thereof may be printed or otherwise reproduced in any material form whatsoever without the author's prior written permission.

.....  
date

.....  
Yonathan Hary H.  
Master of Science



*I dedicate this to my favorite geologist ever, my mom!*



# Acknowledgements

So long and thanks for all the fish.

Douglas Adams



# **Preface**

This dissertation is original work by the author, Yonathan Hary Hutagalung.



# Contents

<b>Acknowledgements .....</b>	<b>xv</b>
<b>Preface .....</b>	<b>xvii</b>
<b>Contents.....</b>	<b>xxix</b>
<b>List of Figures .....</b>	<b>xxi</b>
<b>List of Tables .....</b>	<b>xxiv</b>
<b>List of Abbreviations .....</b>	<b>xxvi</b>
<b>List of Symbols .....</b>	<b>xxviii</b>
<b>1 Introduction .....</b>	<b>30</b>
1.1       Overview .....	30
1.2       Location background.....	31
1.2.1   Iceland Geology .....	31
1.2.2   Reykjanes Peninsula Geology .....	31
1.3       Reservoir Modelling.....	33
1.3.1   TOUGH2 .....	33
1.3.2   AUTOUGH2, PyTOUGH and TIM.....	33
1.3.3   MINC Model .....	34
1.4       Pressure Transient Analysis .....	35
<b>2 Methods .....</b>	<b>36</b>
2.1       Fieldwork observations and interpretations .....	36
2.1.1   Fieldwork Locations.....	36
2.1.2   Small Scale observations.....	37
2.1.3   Medium-Scale observations .....	37
2.2       Numerical Model construction.....	39
2.2.1   Numerical model geometry .....	39
2.2.2   Model Setup .....	42
2.2.3   MINC Model Setup and effect on pressure transient .....	45
2.3       Analytical Model.....	46
2.3.1   Theis solution for constant rate test.....	46
2.3.2   Analytical solution for model setup .....	49
<b>3 Results.....</b>	<b>50</b>
3.1       Radial model result.....	50
3.1.1   Single porosity model.....	50
3.1.2   MINC Model .....	51
3.2       2D Rectangular model result.....	53
3.3       3D Rectangular model result.....	53
3.4       3D Rectangular wavy model result .....	54

<b>4 Analysis and Discussion .....</b>	<b>57</b>
4.1        Radial Model .....	57
4.2        2D Rectangular Model .....	59
4.3        3D Rectangular Model .....	61
4.4        3D Rectangular Wavy Model.....	62
4.4.1    The amplitude impact on injection pressure .....	62
4.4.2    Number of wave impact on injection pressure.....	63
4.4.3    The Volume impact on injection pressure.....	64
4.4.4    Geometry effect on Mass flow direction.....	66
<b>5 Conclusion and Future Works .....</b>	<b>71</b>
5.1        Conclusion.....	71
5.2        Future Work .....	71
<b>Appendix A: Code .....</b>	<b>72</b>
<b>A.1. Code for MINC making. ....</b>	<b>72</b>
<b>A.2. Script for Refining Geometry .....</b>	<b>73</b>
<b>A.3. Script for optimize the Geometry.....</b>	<b>74</b>
<b>A.4. Code for Generating Radial Model.....</b>	<b>75</b>
<b>A.5. Code for converting .LISTING to CSV .....</b>	<b>78</b>
<b>A.6. Code to plot semilog graph .....</b>	<b>78</b>
<b>A.7. Pressure Transient Analysis .....</b>	<b>79</b>
<b>A.8. Modern Theis Analytical Solution .....</b>	<b>83</b>
<b>Appendix B.1 Wavy Model geometries.....</b>	<b>85</b>
<b>References.....</b>	<b>92</b>

# List of Figures

Figure 1.2.1 Main tectonic zone of Iceland .....	31
Figure 1.2.2 Volcanic system in Reykjanesskagi peninsula based on aeromagnetic map. (Sæmundsson et al., 2020).....	32
Figure 1.2.3 Geological map of Reykjanes Peninsula.....	32
Figure 1.3.1 AUTOUGH2 Workflow.....	33
Figure 1.3.2 MINC Model Concept.....	34
Figure 1.4.1 Typical Pressure Transient analysis result for IARF .....	35
Figure 2.1.1 Map of the fieldwork conducted in Reykjanes peninsula .....	36
Figure 2.1.2 Basaltic outcrop found in Hafnarfjordur .....	37
Figure 2.1.3 the sketch of outcrop found in Hafnarfjordur .....	37
Figure 2.1.4 Outcrop found in Helguvik. ....	38
Figure 2.1.5 Sketch of the outcrop found in Helguvik. ....	38
Figure 2.2.1 Numerical model schematic. ....	39
Figure 2.2.2 Radial model grid. ....	40
Figure 2.2.3 Rectangular model grid. ....	40
Figure 2.2.4 Boundary Condition of rectangular model. ....	41
Figure 2.2.5 Cross section of 3D rectangular model .....	41
Figure 2.2.6 boundary condition cross section of rectangular model.....	42
Figure 2.2.7 Radial model setup. ....	43
Figure 2.2.8 2D rectangular model setup. ....	43
Figure 2.2.9 3D rectangular model setup. ....	43
Figure 2.2.10 3D Rectangular Model with Wave Cases. ....	44
Figure 2.2.11 Comparison of single porosity and MINC model on PTA. ....	45
Figure 3.1.1 Pressure profile at injection block of radial model. ....	50
Figure 3.1.2 Pressure transient analysis graph of the radial model. ....	51
Figure 3.1.3 Comparison between radial numerical and analytical model. ....	51
Figure 3.1.4 Pressure profile of Radial MINC model at Injection block. ....	51
Figure 3.1.5 Pressure transient framework of Radial MINC Model. ....	52
Figure 3.1.6 Comparison of Analytical and Numerical model for Radial MINC Model....	52
Figure 3.2.1 Pressure profile of 2D Rectangular model at Injection block. ....	53
Figure 3.3.1 Pressure profile of 3D rectangular model at Injection block. ....	53
Figure 3.4.1 Pressure profile of wavy case 1 at injection block .....	54
Figure 3.4.2 Pressure profile of wavy case 2 at injection block .....	54
Figure 3.4.3 Pressure profile of wavy case 3 at injection block. ....	55
Figure 3.4.4 Pressure profile of wavy case 4 at injection block. ....	55
Figure 3.4.5 Pressure profile of wavy case 5 at injection block. ....	56
Figure 3.4.6 Pressure profile of wavy case 6 at injection block. ....	56
Figure 4.1.1 Mass flow at injection well and neighboring block for non-MINC (a) and MINC (b) model .....	57
Figure 4.1.2 Early wellbore effect at Non-MINC (a) and MINC (b) model .....	57
Figure 4.1.3 Pressure profile of radial and radial MINC. ....	58
Figure 4.1.4 Mass flow at connection between injection well and neighboring block in Non- MINC and MINC model.....	58
Figure 4.1.5 Mass flow of the Injection block for MINC Model .....	58

Figure 4.1.6 Pressure transient analysis for non-MINC (a) and MINC (b) Model .....	59
Figure 4.2.1 Pressure profile of 2D rectangular and radial model at injection block.....	59
Figure 4.2.2 The mass flow direction of rectangular 2D model.....	60
Figure 4.2.3 Mass flow comparison between the Non MINC and MINC model.....	60
Figure 4.3.1 The pressure profile at injection block of 2D and 3D Rectangular model.....	61
Figure 4.3.2 Mass flow direction of the 3D rectangular model.....	61
Figure 4.3.3 The mass flow at injection block of 3D rectangular model. ....	61
Figure 4.4.1 Pressure profile at injection block for 1 wave.....	62
Figure 4.4.2 Pressure profile at Injection block for 2 waves.....	62
Figure 4.4.3 Pressure profile at injection block for 3 waves. ....	63
Figure 4.4.4 Pressure profile at injection block of model with 0.5m amplitude. ....	63
Figure 4.4.5 Pressure profile at injection block of model with 1m amplitude. ....	64
Figure 4.4.6 Pressure profile at injection block for flat rectangular model with different volume. ....	65
Figure 4.4.7 The pressure profile of wavy model compared with the flat model with same number of blocks. ....	65
Figure 4.4.8 Mass flow direction of Case 1 at Injection block cross section .....	66
Figure 4.4.9 Mass flow direction of Case 2 at Injection block cross section .....	67
Figure 4.4.10 Mass flow direction of Case 3 at Injection block cross section. ....	67
Figure 4.4.11 Pressure cross section of the wave structure of Case 3. ....	67
Figure 4.4.12 Mass flow direction of Case 4 at Injection block cross section. ....	68
Figure 4.4.13 Pressure cross section of the wave structure of Case 4. ....	68
Figure 4.4.14 Mass flow direction of Case 5 at Injection block cross section. ....	68
Figure 4.4.15 Pressure cross section of the wave structure of Case 5. ....	69
Figure 4.4.16 Mass flow direction of Case 6 at Injection block cross section. ....	69
Figure 4.4.17 Pressure cross section of the wave structure of Case 6.....	70
Figure 4.4.18 Modified Case 5 and 6 cross section with mass flow arrow. ....	70
Figure 4.4.19 Comparision between the initial and modified Case 5 and 6.....	70



## List of Tables

Table 1 Fixed parameters of the model .....	42
Table 2 3D rectangular model cases.....	43
Table 3 Unit for constant rate well test .....	49
Table 4 Analytical model setup.....	49
Table 5 Number of blocks for every model.....	64



## List of Abbreviations

MSc	Masters of Science
TIM	This Is'nt Mulgraph
VZ	Volcanic Zone
PyTOUGH	Python TOUGH
EOS	Equation of State
2D	Two-dimensional
3D	Three-dimensional
IARF	Infinite Acting Radial Flow



## List of Symbols

Symbol	Description	Unit
$E_1$	Exponential Integral	-
$\rho$	density	$\text{kg/m}^3$
$\infty$	Infinity	-
$\phi$	Porosity	%
$\nu$	Kinematic viscosity	$\text{m}^2/\text{s}$



# Chapter 1

## Introduction

### 1.1 Overview

This thesis aims to initiate an investigation into different geometry found in permeable zone that exist at contact between basaltic lava flow with the example from basaltic rock located in Northern Reykjanes peninsula using the reservoir simulator AUTOUGH2. This also includes developing workflow to conduct this type of research. The initial hypothesis of the research was that these structures would influence the response of the reservoir to fluid injection, in terms of the pressure response. The challenge of this project is to design a model which captures the reservoir characteristics determined from field work. Initially, more field work was planned to use drones to capture the surface geometry which could easily manipulated using leapfrog software and converted into TOUGH2 file. However, due to the harsh winter and the ground mostly covered in snow during this period, this plan was cancelled. Hence, the research was conducted using synthetic surface.

The structure of this thesis is divided into five chapters. The first chapter aims to give an overview of the thesis and literature review including the location background, numerical modelling, and brief explanation of pressure transient analysis. The second chapter explains the fieldwork, geometry, model setup, MINC method, and analytical model. The third chapter provides the results from the reservoir simulation that is plotted in semi log plot, while chapter four explains and discusses the result. The last chapter dedicated to conclusion and potential future work. The thesis also includes appendixes which show the python script used in the research.

In summary, the research objective is to investigate whether different geometry affects the pressure response of isothermal injection while also providing structured workflow which are suitable for the future researcher to continue the development of similar topic and / or for researcher to build more complexity into this research.

## 1.2 Location background

### 1.2.1 Iceland Geology

Iceland, geographically located in between Greenland and Europe. Geologically located in northern part of Atlantic Mid Ocean Ridge which is an extensional zone expanded 1-2 cm/year with a crust thickness of 35 km approximately started forming during the mid Miocene / 20 million years ago due to combination of mantle plume and spreading plate boundaries (Fraedrich & Heidari, 2019). Main volcanic spreading zone in Iceland including the Eyjafjörður Deep, Northern VZ, Grímsvötn-Kverkfjöll VZ, Eastern VZ, Western VZ, Reykjanes Ridge (RR), and Hofsjökull VZ which shown in Figure 1.2.1(Sæmundsson et al., 2020).

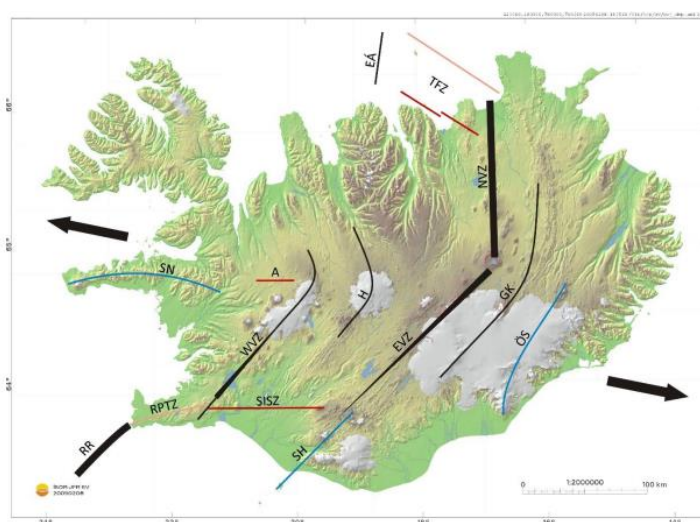


**Figure 1.2.1 Main tectonic zone of Iceland**

The lithology of Iceland composed of predominantly basaltic features such as lava flow, pillow basalt, and intrusion with some minor rhyolitic and intermediate volcanism present (Scott et al., 2022). Hyaloclastite, a volcaniclastic rock formed as product of lava contact with water ice also present in Iceland during the glaciation period (Watton et al., 2013).

### 1.2.2 Reykjanes Peninsula Geology

Reykjanes peninsula located in southwestern part of Iceland is a unique geological region characterized by its primarily basaltic landscape which located in Reykjanes peninsula trans-tensional zone which is an oblique fault formed in mid Atlantic ridge system connecting Western Volcanic Zone and Reykjanes Ridge (Sæmundsson et al., 2020). This results in the formation of numerous fissures, craters, lava fields, and intense geothermal activities. This also resulted in formation of volcanic system including Reykjanes, Svartsengi, Fagradalsfjall, and Krýsuvík systems which shown in Figure 1.2.2 below.

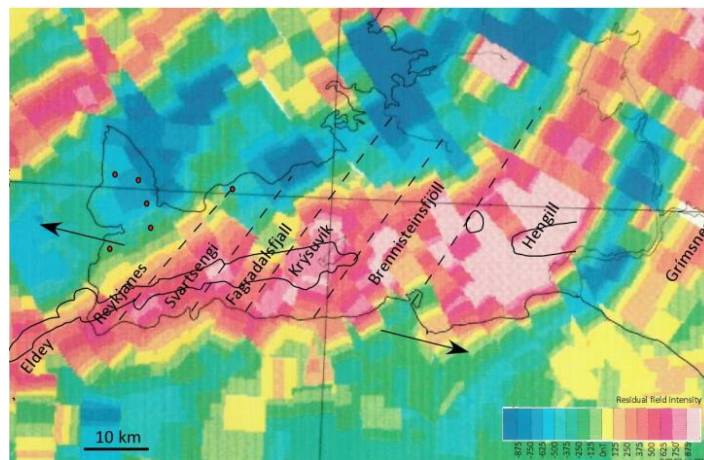


**Figure 1.2.2 Volcanic system in Reykjanes peninsula based on aeromagnetic map.**  
**(Sæmundsson et al., 2020)**

The geology of Reykjanes peninsula is mainly dominated by basaltic rock varies from older than 9000 years old to younger than 900 years ago and minor hyaloclastite deposits. Using map from (ISOR, n.d.), the oversimplified map of Reykjanes peninsula is shown in figure Figure 1.2.3 below.

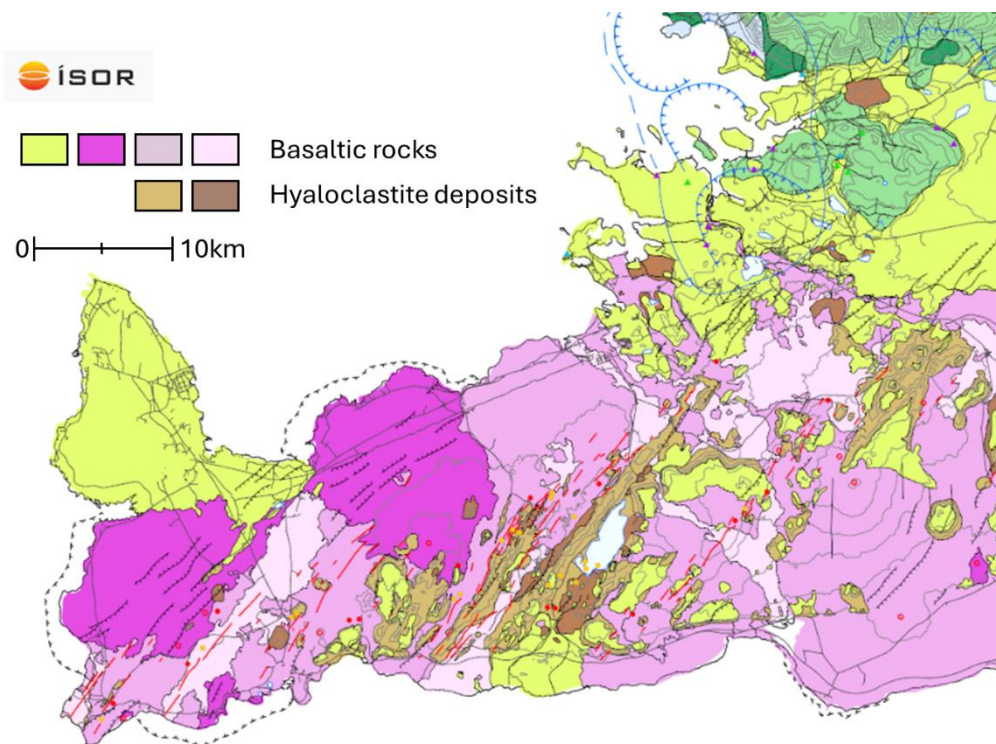


**Figure 1.2.3 Geological map of Reykjanes Peninsula.**

## 1.3 Reservoir Modelling

Geothermal reservoir modelling is an essential tool in many sectors such as geothermal exploration and resource development. According to (Nugraha et al., 2022), the most efficient stages of reservoir modelling starting from making 3D conceptual modelling for the basis of numerical model, choosing appropriate grids, selecting appropriate data for natural state process, history matching with production data, and running the future scenario. The paper also mentions the recommended tools for effective reservoir modelling including AUTOUGH2, PyTOUGH, Leapfrog geothermal, and Waiwera.

### 1.3.1 TOUGH2

TOUGH2 is FORTRAN77 based numerical simulator developed by Lawrence Berkeley National Laboratory used for non-isothermal flows of multicomponent, multiphase fluids in one, two, or three dimensional porous and fractured media which dedicated for geothermal reservoir engineering, nuclear waste disposal, environmental assessment and remediation, and hydrology which firstly introduced to public in 1991. (Pruess et al., 2012)

### 1.3.2 AUTOUGH2, PyTOUGH and TIM.

AUTOUGH2 is modified version of TOUGH2 developed by Auckland University which has additional features compared to TOUGH2 including increased efficiency of memory usage, one simulator for all EOS types and more generation types. (Yeh et al., 2012) Simplified AUTOUGH2 workflow shown in Figure 1.3.1 below.

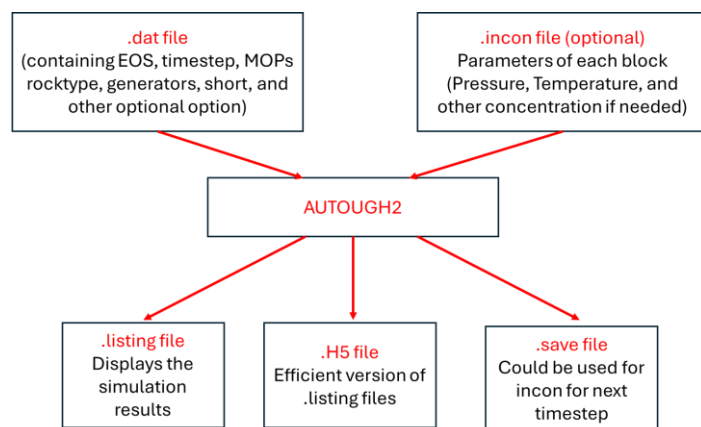


**Figure 1.3.1 AUTOUGH2 Workflow**

PyTOUGH is a set of python package developed in purpose of creating simplicity for manipulating TOUGH2 geometry and data file which also could be used for analyzing and displaying model simulation results. (Croucher, 2023) Auckland university also created graphical user interface based on PyTOUGH called TIM, which is useful for manipulating rocktype, adding generators, and others. (O'Sullivan et al., 2013) Combining these tools, geothermal reservoir modelling would be more practical.

### 1.3.3 MINC Model

Multiple Interacting Continua (MINC) is a method for modelling fluid and heat flow in fractured media developed by (Pruess & Narasimhan, 1985) which adopted from dual porosity method developed by (Warren & Root, 1963). This theory was implemented in TOUGH2 using the sub-gridding method which shown in Figure 1.3.2 below.

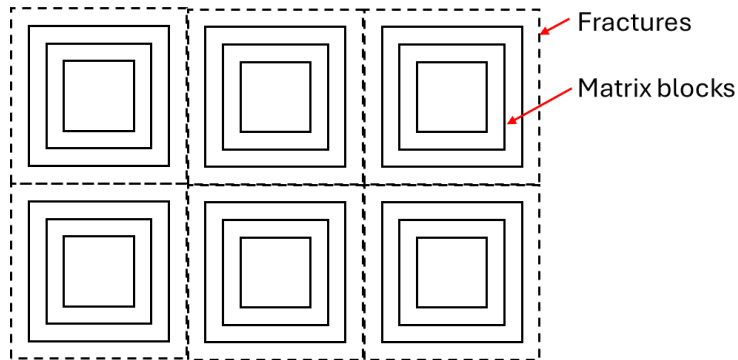


**Figure 1.3.2 MINC Model Concept**

According to research conducted by (O'Sullivan, 1987), the effect of MINC on pressure response mainly affecting the early timestep or mainly in wellbore storage periods due to relatively large volume of well block and interaction between the fracture and the matrix.

## 1.4 Pressure Transient Analysis

Pressure transient analysis (PTA) is the analysis of pressure and flow data set which typically involves model matching either numerically or analytically of a well and reservoir. Main objective of PTA is to obtain information about reservoir, typically includes reservoir transmissivity ( $k_h$ ), skin factor ( $s$ ), initial reservoir pressure and might as well has a dual purpose to determine well condition.

There are four main well test types which includes drawdown test, build-up test, injection test, and fall off test. However, to fit the purpose of the thesis only injection test conducted. The definition of injection test is an injection into a static well which theoretically will increase the pressure. There are several methods of analytical graphical methods for pressure transient analysis, including Miller – Dyes – Hutchinson semilog, Horner semilog, multirate superposition plot, two-rate plot, general semilog plot, log-log plot, and Bourdet pressure derivative plot (Zarrouk & McLean, 2019a, p. 4). However, this thesis focused on Miller – Dyes – Hutchinson semilog and Bourdet pressure derivative plot.

The typical pressure transient analysis results for infinite acting and two-dimensional radial flow on well horizontally shown in figure below. (Zarrouk & McLean, 2019b, p. 8) The characteristic including flat derivative during IARF and pressure derivative have unit slope during wellbore storage period.

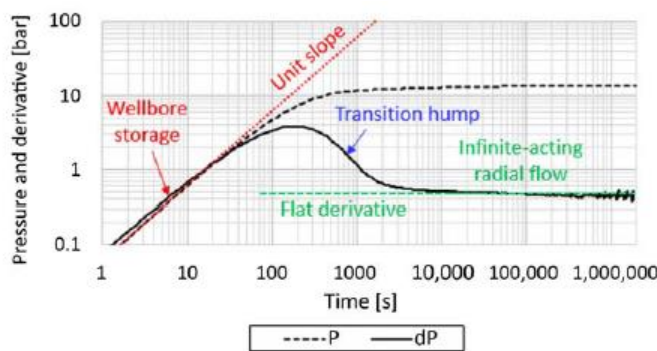


**Figure 1.4.1 Typical Pressure Transient analysis result for IARF**

# Chapter 2

## Methods

The methodology of the research combines fieldwork, discussion, analytical methods, and numerical modelling. The field work was conducted in three area including Hafnarfjordur, Hvassahraun, and Helguvik to observe the basaltic rock geological properties. Originally, drone measurement was supposed to be conducted. However, it was cancelled due to harsh winter conditions in the area. The analytical model conducted in the research is theis solution for constant rate test which is used to validate the radial numerical model. The numerical model in this research includes radial model, 2D rectangular model and 3D rectangular model.

### 2.1 Fieldwork observations and interpretations

#### 2.1.1 Fieldwork Locations

The field work started in Hafnarfjordur near the aluminum smelter which aims to collect the data of small-scale features continued by Hvassahraun and Helguvik. Field work was also conducted near Kleifarvatn to observe the hyaloclastite. However, the visit was inconclusive. Field work conducted in four different areas marked with red dot with the Helguvik circled since this is focus of the thesis as shown in Figure 2.1.1 below.

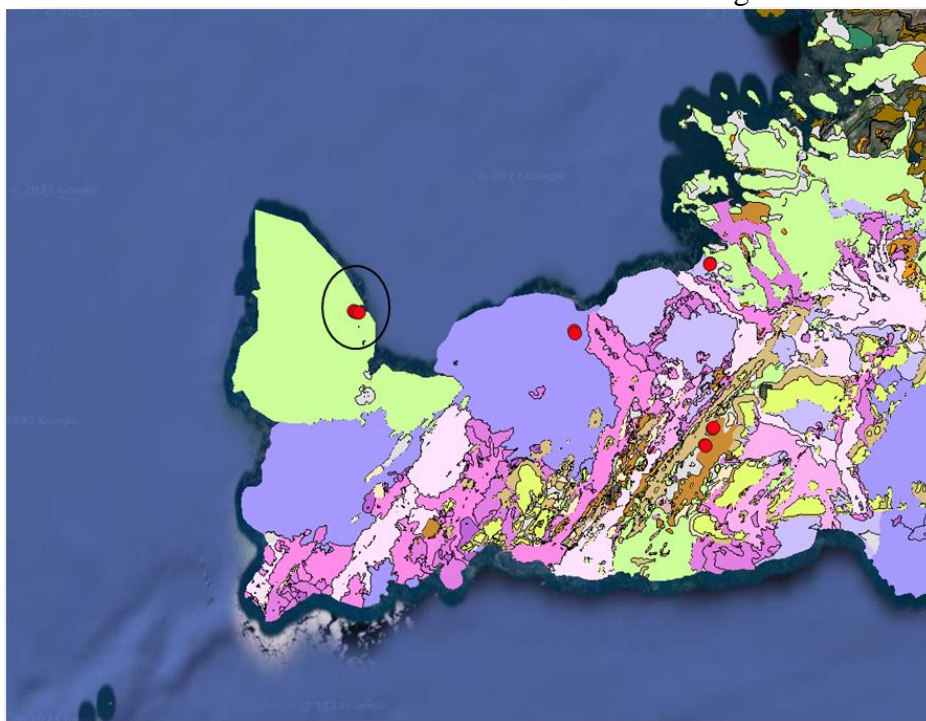


Figure 2.1.1 Map of the fieldwork conducted in Reykjanes peninsula

### 2.1.2 Small Scale observations

The small-scale outcrop was found in Hafnarfjordur which was chosen as the representative of basaltic rocks that were observed in northern Reykjanes peninsula as shown in Figure 2.1.2 below.



**Figure 2.1.2 Basaltic outcrop found in Hafnarfjordur**

Using this observation, the sketch was made as shown in Figure 2.1.3Figure 2.1.3 below.

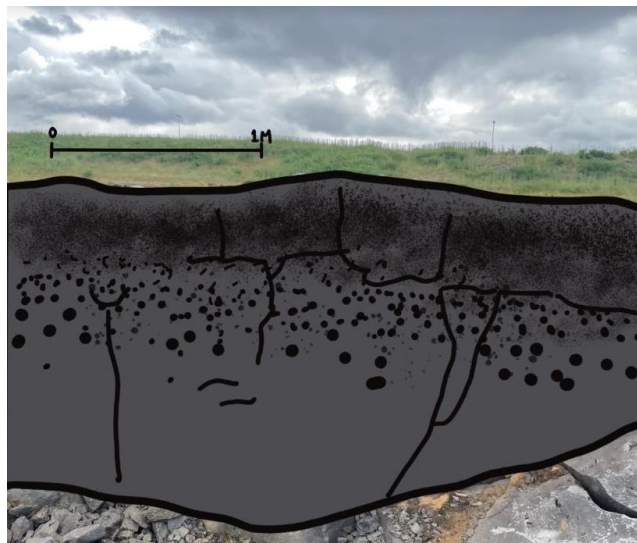


**Figure 2.1.3 the sketch of outcrop found in Hafnarfjordur**

The interpretation of the outcrop is the top layer of the basaltic layer has a vesicularity ranging from 1mm to 10mm with fracture spacing on average of 15cm. The lower section of the lava flow has vesicularity ranging from 1 to 60 mm with less intensity compared to the upper section and a fracture spacing of 40-100cm with occasional 20cm range.

### 2.1.3 Medium-Scale observations

After the Hafnarfjordur visit, the next stop including Hvassahraun and Helguvik which could be concluded that the lava flow has very similar structure as shown at picture (a) on

the left which means this could be applied on the medium structure which shown in picture (b).

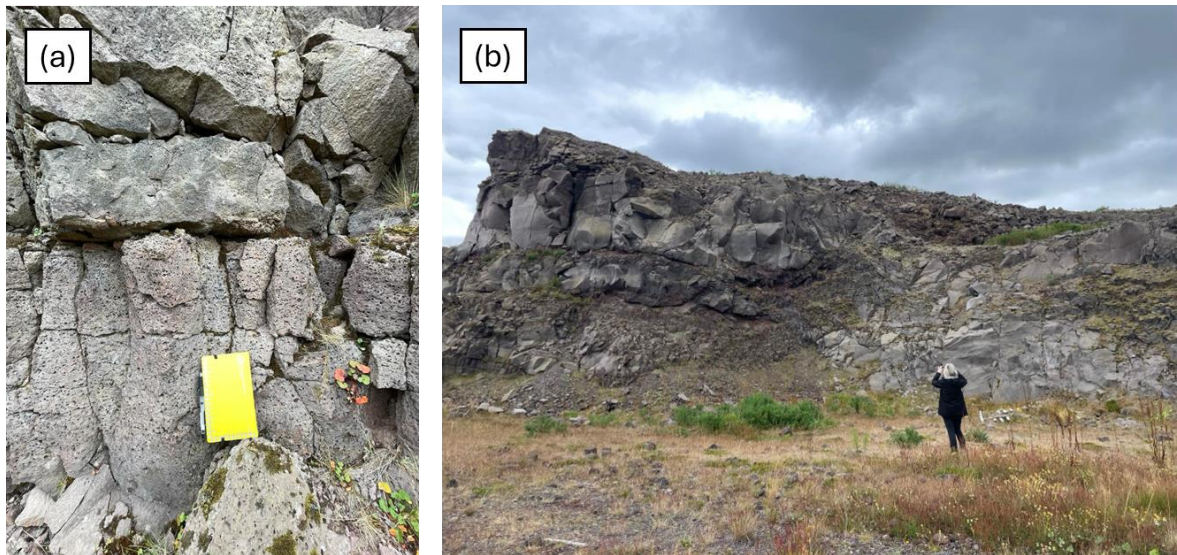


**Figure 2.1.4 Outcrop found in Helguvik.**

The observation that could be concluded after the observation is the medium scale structure in Helguvik has similar vertical textural structure as the small-scale features, massive, has wavy surface which has amplitude of around 2 to 10 m, and has breccia layer on top of the features. With this observation, the sketch was drawn as shown in Figure 2.1.5 below.

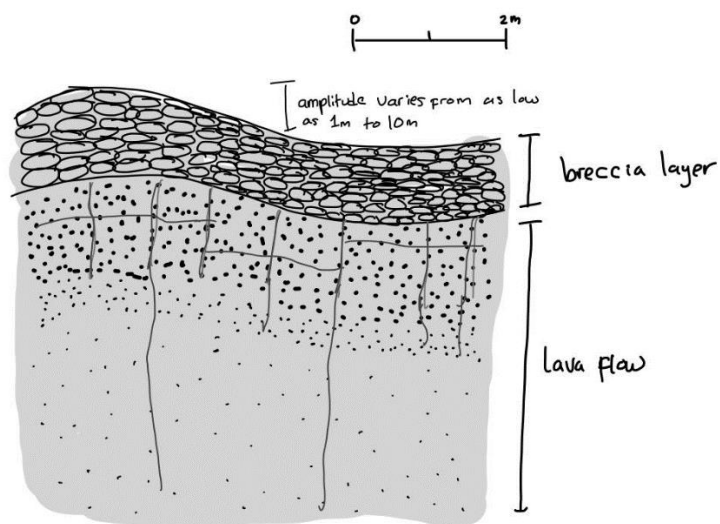


**Figure 2.1.5 Sketch of the outcrop found in Helguvik.**

## 2.2 Numerical Model construction

The numerical modelling concept of the research was building complexity. Modelling started by constructing the 2D rectangular model which is a single 0.25 m layer that has infinite boundaries. Using the same volume in injection block, the radial model was constructed. The radial model was constructed to conduct the analytical Theis solution, pressure transient analysis, and used to validate the 2D rectangular model results. Using the 2D rectangular model, the same 3D rectangular model was constructed which one reservoir layer boundaries with impermeable boundaries. The wavy surface then constructed which is a modified version of the 3D rectangular model that was created. The wavy surface has 6 different cases with different wavelengths and amplitudes. After all the models were created, MINC model with 2 fractures set and 2 matrix block was created in the boundary conditions of the model. The scheme of the numerical model is shown in Figure 2.2.1.



**Figure 2.2.1 Numerical model schematic.**

### 2.2.1 Numerical model geometry

The main objective of radial model construction is to validate the reasonableness of the 2D rectangular model. The radial model could be validated using infinite-acting radial flow (IARF) on pressure transient analysis and constant rate test analytical model. Hence, the radial model could be a very reliable benchmark for this.

The radial model was created to have a volume of the center block as similar to the 2D rectangular model injection block which could easily controlled by using the similar radius, thickness, and well volume. The model was designed to have 49 logarithmically short-spaced blocks to represent the skin continued by 100 logarithmically long-spaced blocks to avoid the boundary effect which is up to approximately 20km. The upper and lower boundaries closed with every block has thickness of 0.25m. The concept graphically drawn in figure 2.2.2. below

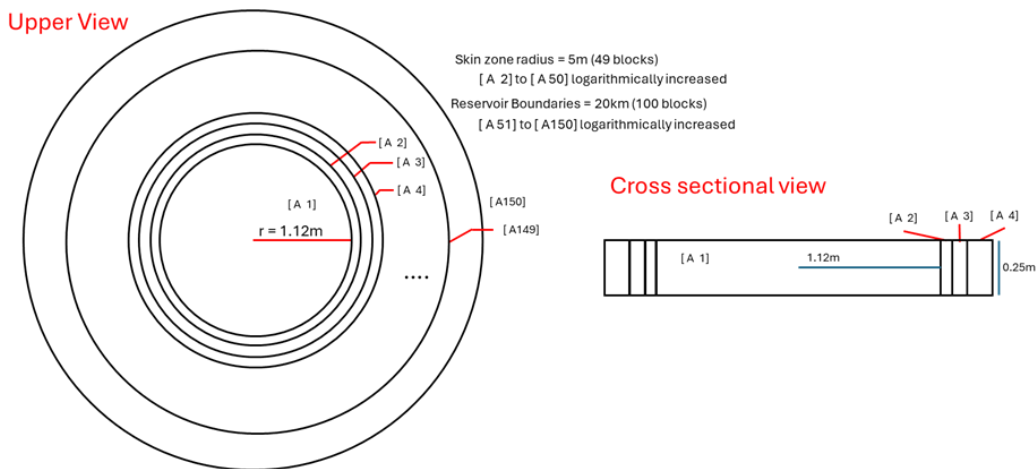


**Figure 2.2.2 Radial model grid.**

The radial model was constructed using PyTOUGH script which could be generated using **Appendix A.4**. There is a slight problem with running the controlled time-stepping of the model using this script. Hence, the manual input was advised to control the time-step which is also explained in the appendix.

The 2D rectangular model was constructed to proceed with the principle of building complexity of the model. This acts as a bridge to validate the reliability of the model with radial model and building more complex 3D rectangular model. The 2D rectangular model geometry was created using PyTOUGH script with a closed boundary and thickness of 0.25m to match with the radial model.

The geometry creation started by using a 20 km x 20 km grid with each block sized 2 km x 2 km which refined 11 times using **Appendix A.2** until it reaches a boundary condition is 36 m x 36 m with each block in boundary condition is around 2.4m x 2.4 m in size. The size was chosen since it was the best size to represent the intermediate size block without overcomplex and adding unnecessary run time. In every refinement, it is advised to optimize the grid to provide a tidy outcome using **Appendix A.3**. The full-scale of rectangular grid shown in Figure 2.2.3.

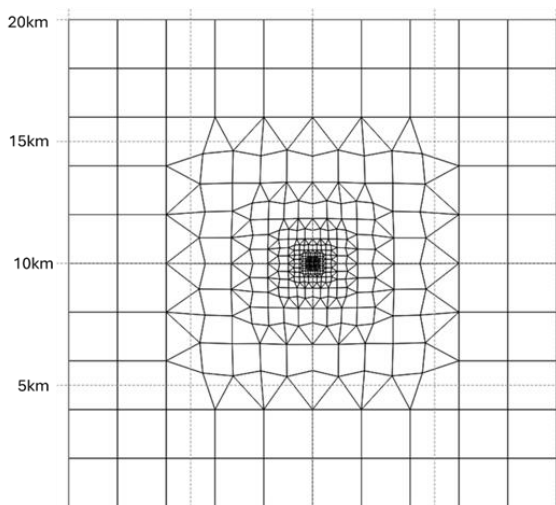


**Figure 2.2.3 Rectangular model grid.**

The boundary condition scaled rectangular model shown in Figure 2.2.4 below.

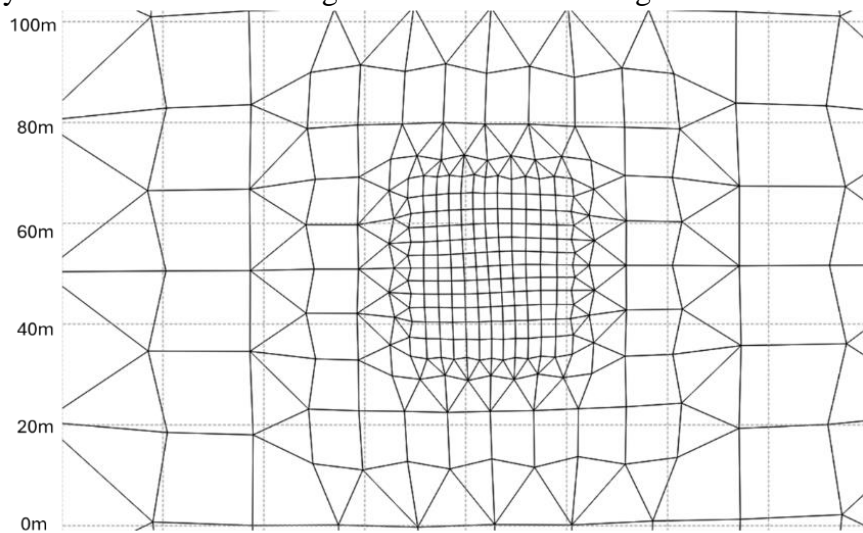


**Figure 2.2.4 Boundary Condition of rectangular model.**

The 3D model was created using the same script as the 2D rectangular model to improve the complexity without changing the x and y geometry of the model. The approach of constructing the 3D rectangular model was decreasing the thickness of each block as it goes to the center of the model. This decision was made to create an appropriate space to develop a wavy structure which is the main purpose of the research. By decreasing the block consistently from 20 m to 0.25, this prevents the thermodynamic error that commonly occurs on TOUGH2 simulator when abruptly changes the geometry thickness.

The cross section of 3D model shown Figure 2.2.5 in below. The same as 2D rectangular model, the boundary goes to 20 x 20 km which could be considered as infinite extent with no boundary effect present.

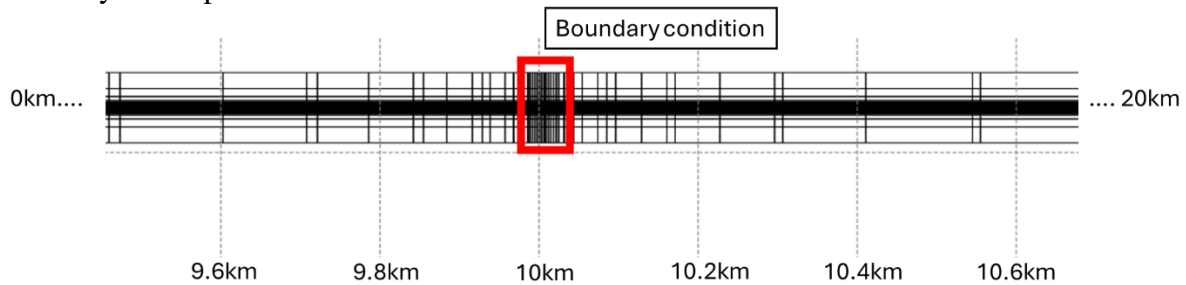


**Figure 2.2.5 Cross section of 3D rectangular model**

For the 3D model, the boundary condition cross section of each model at smallest model extent shown in Figure 2.2.6 below.

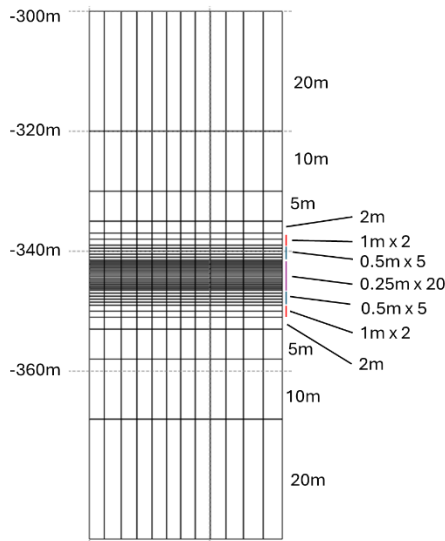


**Figure 2.2.6 boundary condition cross section of rectangular model**

## 2.2.2 Model Setup

The fixed parameters for all the numerical models are shown below.

**Table 1 Fixed parameters of the model**

Parameters	Measure with unit
Reservoir Temperature	10°C
Reservoir Pressure	34.798 bar
Reservoir Permeability	$5 \times 10^{-13}$
Reservoir Porosity	0.25 / 25%
Injection block thickness	0.25m
Injection block volume	$\sim 1.72 \text{ m}^3$
Injection Temperature \ Enthalpy	10°C (Isothermal) / Simulation type: 1 1 2 6 W
Injection Mass flow	0.5 kg/s
Injection time	$10^7$ seconds / 0.32 years
Boundary condition porosity	0.01 %
Boundary condition permeability	$1 \times 10^{-16}$

The reservoir pressure and temperature were chosen at the value of 34.798 bar and 10°C because the assumption was the injection conducted in relatively cold reservoir with around 320 m to 360 m in depth. The isothermal single water simulator was chosen to provide a stable temperature profile, where the injection mass flow and injection time was chosen to provide a substantial amount of pressure response without adding additional unnecessary simulator run-time. The boundary conditions permeability and porosity values were chosen to provide a relatively impermeable boundary effect to the model.

As explained in geometry setup, the injection conducted in the center of the well with a closed top and lower boundary. Hence, the flow of the fluid will be spread radially. The illustration of the radial model shown in Figure 2.2.7 below.

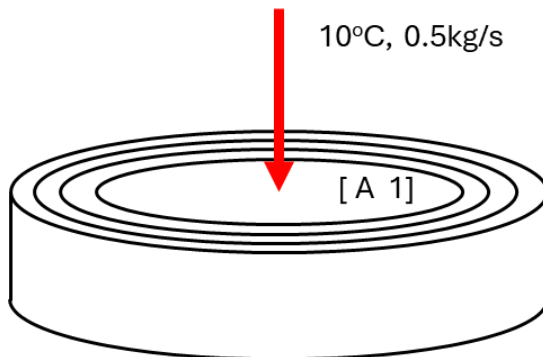


**Figure 2.2.7 Radial model setup.**

As explained in the geometry section, the 2D rectangular model extends up to 20 km which represents the infinite boundary. The purpose of creation of this model is to make the model as similar as radial model which has infinite boundary and closed top and bottom. Hence, this could easily be matched with the radial model. The illustration of the 2D rectangular model shown in Figure 2.2.8 below.

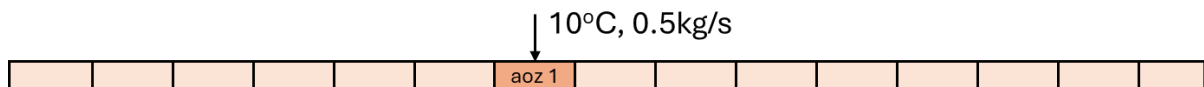


**Figure 2.2.8 2D rectangular model setup.**

The first 3D rectangular model that was created has the same perimeter as the 2D rectangular model to see the difference between the truly closed boundary and relatively impermeable boundary before building more complexity in wavy model creation. The illustration of the 3D rectangular model shown in Figure 2.2.9 below.

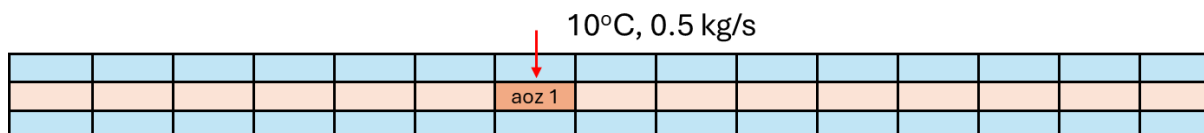


**Figure 2.2.9 3D rectangular model setup.**

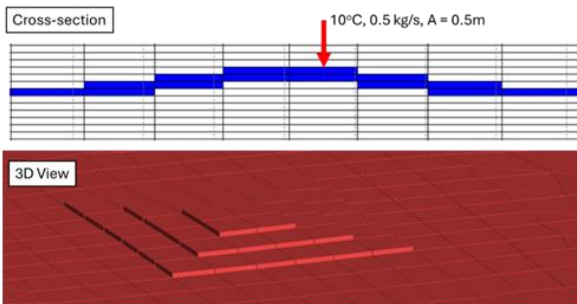
After validating the radial model, 2D rectangular model, and 3D rectangular model, the 3D rectangular wavy model created which has 6 different cases with different number of wave and amplitude which are explained in Table 2 below.

**Table 2 3D rectangular model cases**

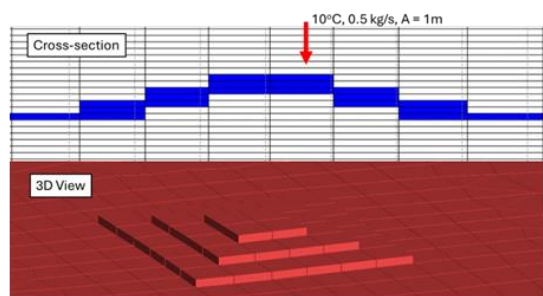
Case number	#Wave	Amplitude
1	1	0.5 m
2	1	1 m
3	2	0.5 m
4	2	1 m
5	3	0.5 m
6	3	1 m

The 3D Rectangular model with wave shown in figure below and the larger version could be found in **Appendix B.1**.

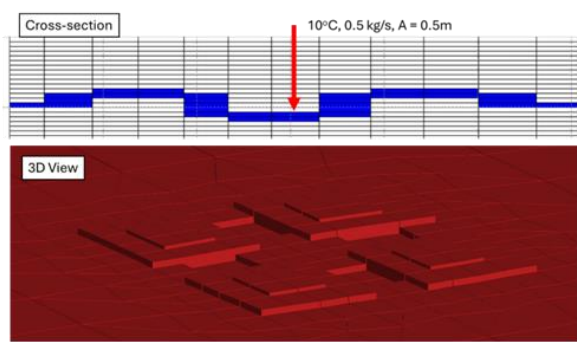
Case 1



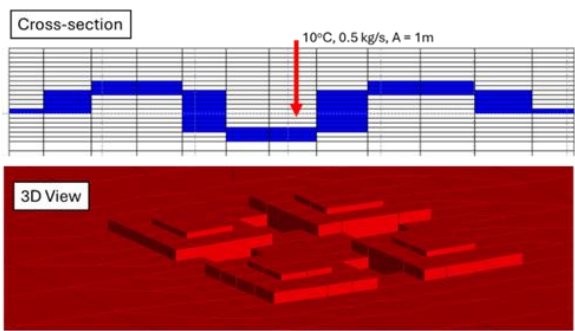
Case 2



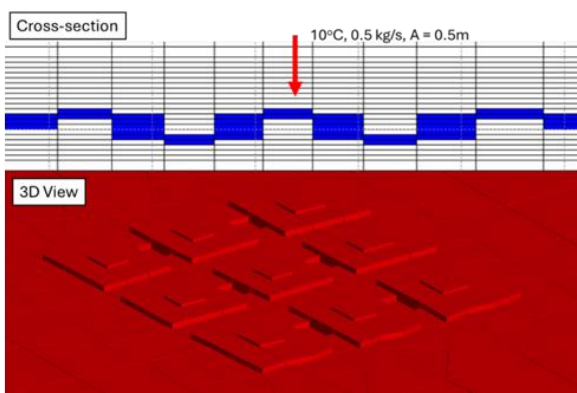
Case 3



Case 4



Case 5



Case 6

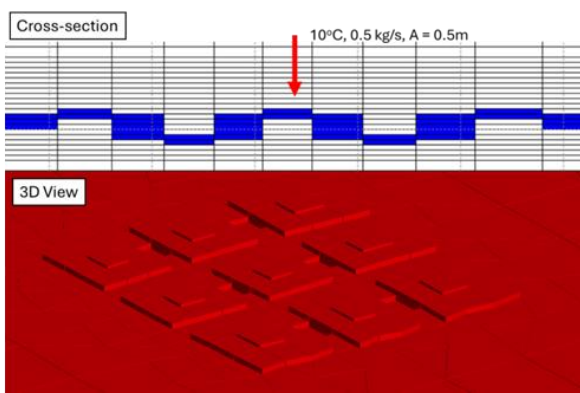
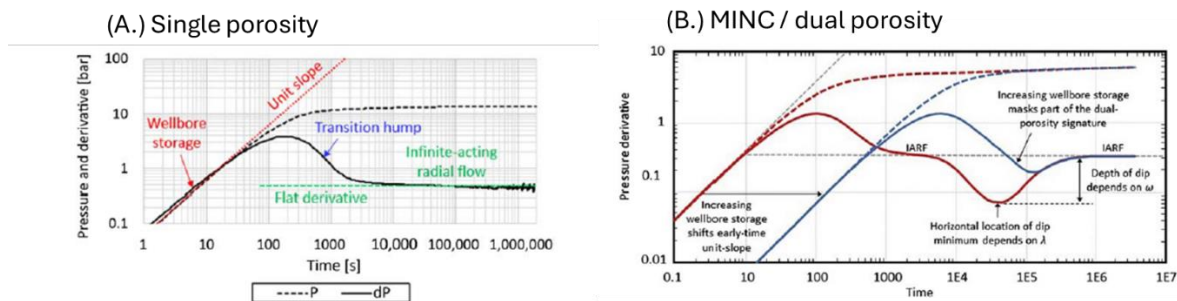


Figure 2.2.10 3D Rectangular Model with Wave Cases.

### 2.2.3 MINC Model Setup and effect on pressure transient

The MINC Model was created to provide an actual representation of the fluid flow in a rock of reservoir. The MINC Model has been constructed in every model and each of them has 2 fracture sets and 2 matrixes with lower permeability  $5 \times 10^{-15}$ . The MINC Block applied in the boundary conditions and strictly applied at reservoir rock type. The script for generating MINC model is available in [Appendix A.1](#).

According to (Zarrouk & McLean, 2019b), the MINC model has a characteristic on pressure derivative plot. The first reservoir response is from the fractures as they have greater transmissivity and are connected directly to the wellbore. After some period, the primary porosity in the matrix will begin to respond, flowing into fractures and causing the pressure derivative to dip, then finally come back to straight line infinite acting radial flow. In the Miller – Dyes – Hutchinson semilog plot, this could be determined by the slight hump at early timestep. The typical result of single porosity and MINC model is shown in Figure 2.2.11 below.



**Figure 2.2.11 Comparison of single porosity and MINC model on PTA.**

## 2.3 Analytical Model

The analytical model used in the experiment is theis solution for constant rate test which has purpose to validate the radial numerical model. Theis solution introduced in 1935 introduced to determine the hydraulic properties including transmissivity and storativity of nonleaky confined aquifers which performed by matching theis type curve to drawdown data plotted on logarithmic axes. (Theis, 1935)

### 2.3.1 Theis solution for constant rate test

Theis solution modified for the analysis of simple constant rate injection test in isothermal reservoir with assumption that the layer feeding the well is horizontal, constant thickness, uniform with depth and laterally, impermeable at top and bottom, and infinite boundaries extent. (Newson, n.d.)

These assumptions mean that flow is radially symmetric. Then the governing pressure diffusion equation for the reservoir region outside the well is:

$$\frac{\partial p}{\partial t} = D \left( \frac{\partial^2 p}{\partial r^2} + \frac{1}{r} \frac{\partial p}{\partial r} \right) \quad (1)$$

Where diffusivity (D):

$$D = \frac{k/v}{\phi\rho C} \quad (2)$$

For the analysis of constant drawdown test, equation 1 must be solved for  $r_w < r < \infty$ ,  $0 < t < \infty$   
With boundary conditions at the well

$$r = r_w: \quad -2\pi r h \frac{k}{v} \frac{\partial p}{\partial t} = q_m \quad (3)$$

$q_m$  is positive for injection and negative for production. Far from the well boundary condition is:

$$r \rightarrow \infty: \quad p = p_0 \quad (4)$$

Boundary conditions apply for  $0 < t < \infty$ . Initial state of reservoir given by:

$$p = p_0 \quad \text{for } r_w \leq r < \infty \quad (5)$$

The mathematical equation could be solved using Laplace transform (Widder, 1941) which defined by:

$$P(r, s) = \int_0^\infty e^{-st} p(r, t) dt \quad (6)$$

Hence, the transform of equation 1 gives:

$$D \left( \frac{\partial^2 p}{\partial r^2} + \frac{1}{r} \frac{\partial p}{\partial r} \right) = s P - p(r, 0) \quad (7)$$

Using initial condition and rearrangement:

$$\frac{\partial^2 p}{\partial r^2} + \frac{1}{r} \frac{\partial p}{\partial r} = \frac{1}{D} (s P - p_0) \quad (8)$$

Therefore, the solution could also be written as:

$$P = A I_0 \left( r \sqrt{\frac{s}{D}} \right) + B K_0 \left( r \sqrt{\frac{s}{D}} \right) = \frac{q_m}{s}$$

Where  $I_0$  and  $K_0$  are modified Bessel functions.

The transform of boundary conditions at equation 3 and 4 at  $r = r_w$ :

$$\frac{-2\pi r h k}{v} \frac{dP}{dr} = \frac{q_m}{s} \quad (9)$$

And as  $r \rightarrow \infty$ :

$$p = \frac{p_0}{s} \quad (10)$$

Using *equation 10*, first gives  $A = 0$  since  $I_0 \rightarrow \infty$  as  $r \rightarrow \infty$ . Then *equation 9* gives:

$$\frac{2\pi h k}{v} r_w B \sqrt{\frac{s}{D}} K_1 \left( r_w \sqrt{\frac{s}{D}} \right) = \frac{q_m}{s} \quad (11)$$

Approximate the finite but small well radius  $r_w$  by zero and use:

$$\lim_{x \rightarrow 0} x K_1(x) = 1$$

This is an important simplification which allows the problem to be solved analytically. Then *equation 11* gives:

$$B = \frac{q_m}{2\pi r h k / \nu s} \frac{1}{s}$$

Hence, the solution for  $P(r, s)$  is:

$$P = \frac{p_o}{s} + \frac{q_m}{2\pi h k} \frac{1}{s} k_0 \left( r \sqrt{\frac{s}{D}} \right) \quad (12)$$

This could be inverted using:

$$L^{-1}\{K_0(a\sqrt{s})\} = \frac{1}{2t} e^{-\frac{r^2}{4Dt}} dt \quad (13)$$

Comparing the *equation 12* and *13* and using some properties of Laplace transform:

$$p(r, t) = p_o + \frac{q_m}{2\pi h k / n} \int_0^t \frac{1}{2t} e^{-\frac{r^2}{4Dt}} dt \quad (14)$$

The substitution  $z = r^2/4Dt$  simplifies *equation 14*:

$$P = \frac{p_o}{s} + \frac{q_m}{4\pi h k} \int \frac{e^{-z}}{z} dz \quad (15)$$

The definition of exponential integral:

$$E_1(x) = -Ei(-x) = \int \frac{e^{-z}}{z} dz$$

Hence, the equation is:

$$p(r, t) = p_o + \frac{q_m}{4\pi h k} Ei \left( -\frac{r^2}{4Dt} \right) \quad (16)$$

Or in modern notation:

$$p(r, t) = p_o + \frac{q_m}{4\pi h k} E_1 \left( \frac{r^2}{4Dt} \right) \quad (17)$$

This equation could be transformed into useful graph using script in **Appendix A.8**.

Description of symbol and unit shown in table 3 below:

**Table 3 Unit for constant rate well test**

symbol	description	Unit
$p_0$	Initial Pressure	Pa
$q_0$	Flow rate (+ve for inj; -ve for production)	kg/s
$h$	Feedzone thickness	m
$k$	permeability	$m^2$
$\nu$	Kinematic viscosity	$m^2/s$
$E_1$	Exponential integral	
$D$	Pressure diffusivity	$m^2/s$
$\phi$	porosity	%
$\rho$	density	$kg/m^3$
$C$	Compressibility	$Pa^{-1}$

### 2.3.2 Analytical solution for model setup

The parameter used to validate the analytical model shown in table 4 below:

**Table 4 Analytical model setup**

$p_0$	$3.798 * 10^6$ Pa
$h$	0.25 m
$k$	$5 * 10^{-13}$ $m^2$
$\nu$	$1 * 10^{-6}$
$\phi$	0.25
$r$	1.12 m
$\rho$	1000 $kg/m^3$
$C_{rock}$	$1 * 10^{-10}$
$C_{fluid}$	$4.52 * 10^{-10}$
$t$	$10^{-2}$ to $10^7$ s
$q_m$	0.5 kg/s

# Chapter 3

## Results

This section is dedicated to the results of the numerical model and simulation constructed using the geometry and model setup as explained in *chapter 2*. This also includes the pressure transient analysis and analytical model for constant rate test.

### 3.1 Radial model result

#### 3.1.1 Radial model

The pressure response of the injection of 0.5 kg/s water into radial model shown in figure below.

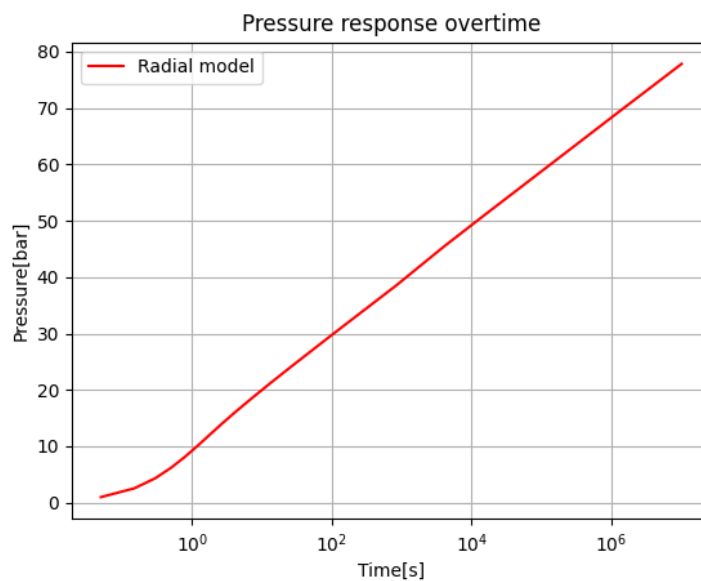


**Figure 3.1.1 Pressure profile at injection block of radial model.**

Using this data, pressure transient conducted and plotted in figure below.

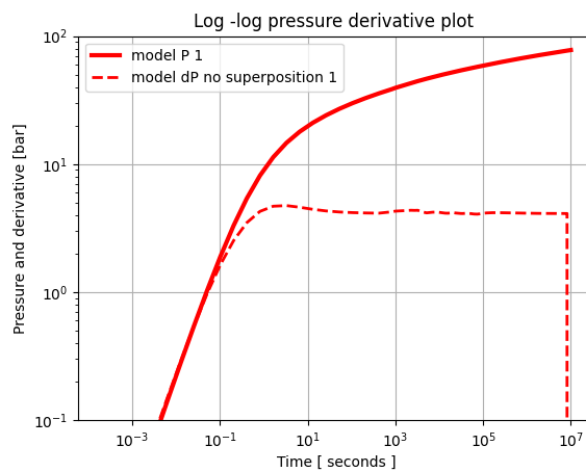


**Figure 3.1.2 Pressure transient analysis graph of the radial model.**

The radial model compared with the analytical model shown in figure below

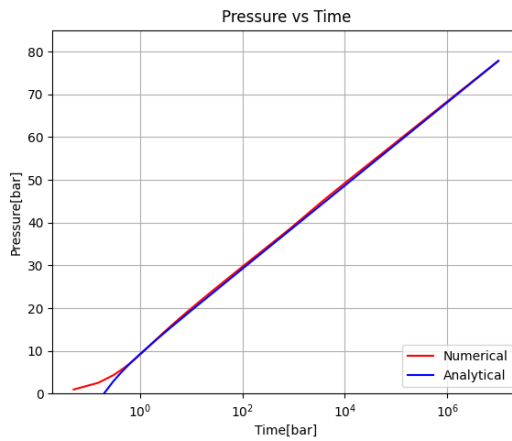


**Figure 3.1.3 Comparison between radial numerical and analytical model.**

### 3.1.2 MINC Model

The pressure profile of radial MINC at injection block shown below.

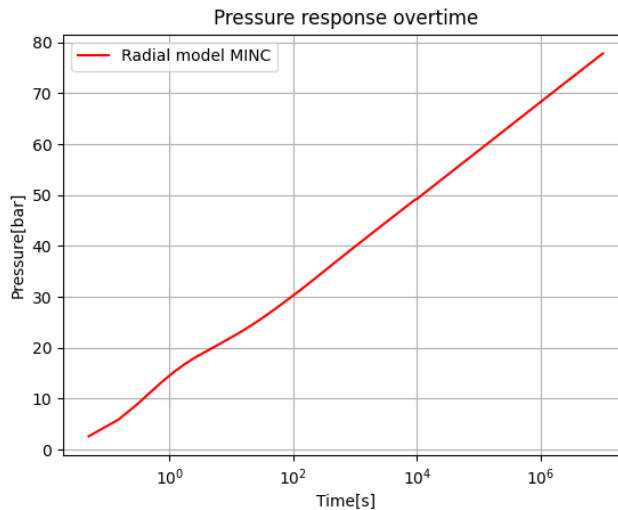


**Figure 3.1.4 Pressure profile of Radial MINC model at Injection block.**

The pressure derivative plot for MINC model shown in figure below

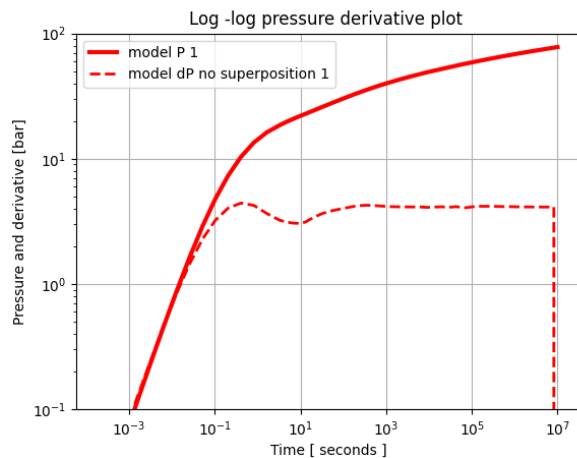


**Figure 3.1.5 Pressure transient framework of Radial MINC Model.**

The MINC Model compared with the analytical solution shown in figure below.

Pressure vs Time

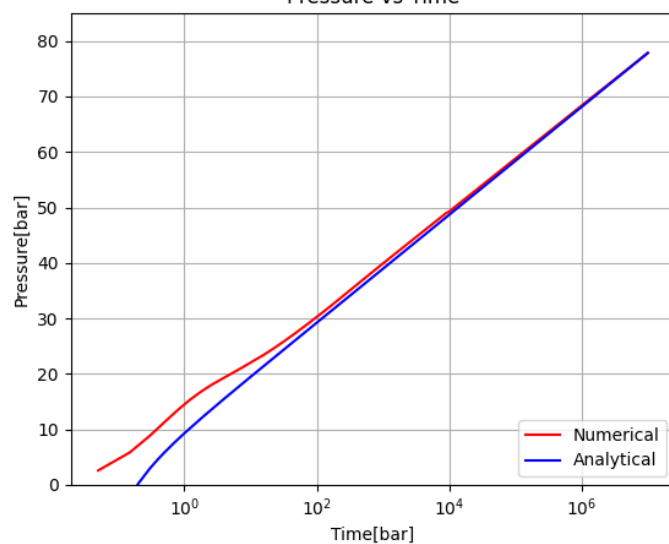


**Figure 3.1.6 Comparison of Analytical and Numerical model for Radial MINC Model.**

## 3.2 2D Rectangular model result

2D Rectangular model pressure profile at injection block shown in figure below

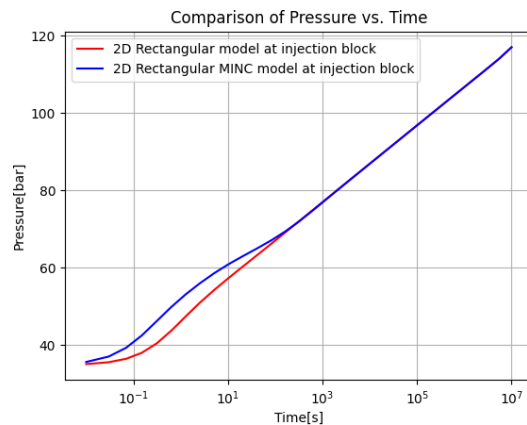


**Figure 3.2.1 Pressure profile of 2D Rectangular model at Injection block.**

## 3.3 3D Rectangular model result

The 2D Rectangular model converted into 3D rectangular model which shown in figure below.

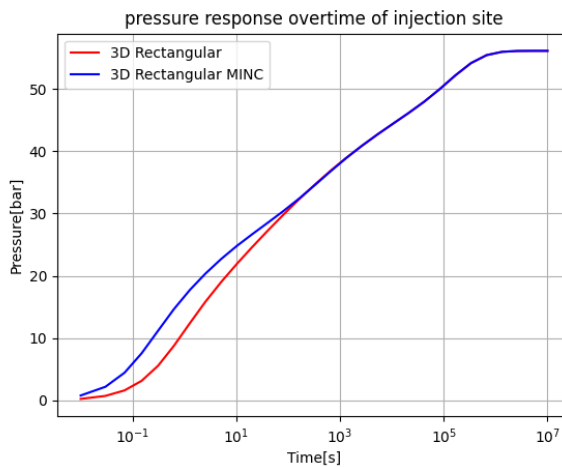


**Figure 3.3.1 Pressure profile of 3D rectangular model at Injection block.**

### 3.4 3D Rectangular wavy model result

The pressure profile at injection block for case 1 of single porosity and MINC model shown in figure below.

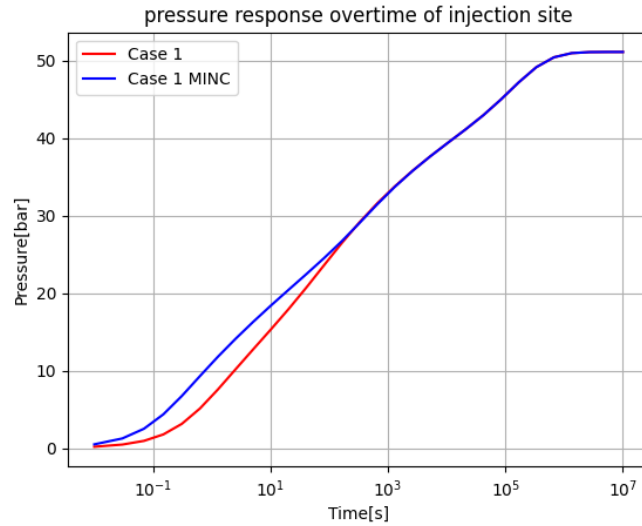


**Figure 3.4.1 Pressure profile of wavy case 1 at injection block**

The pressure profile at injection block for case 2 of single porosity and MINC model shown in figure below.

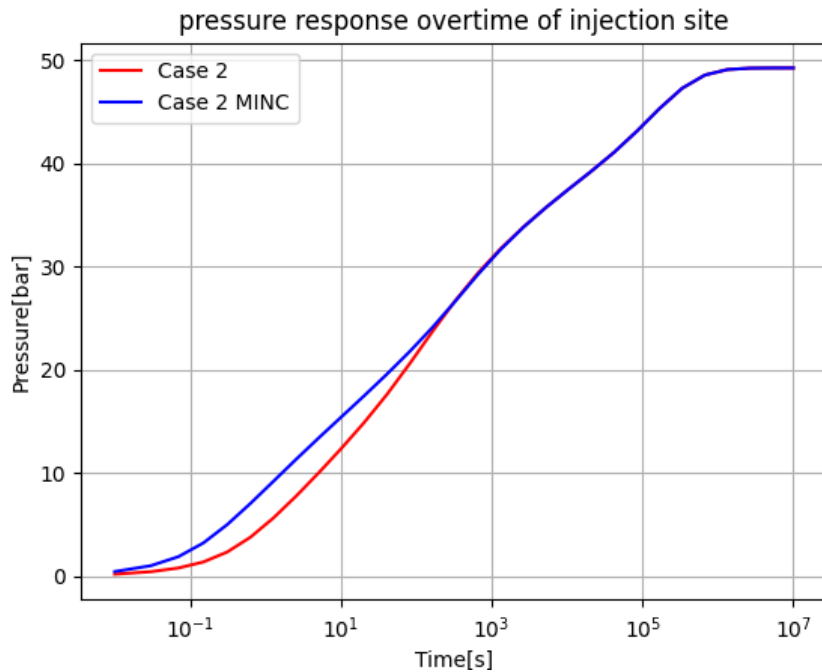


**Figure 3.4.2 Pressure profile of wavy case 2 at injection block**

The pressure profile at injection block for case 3 of single porosity and MINC model shown in figure below.

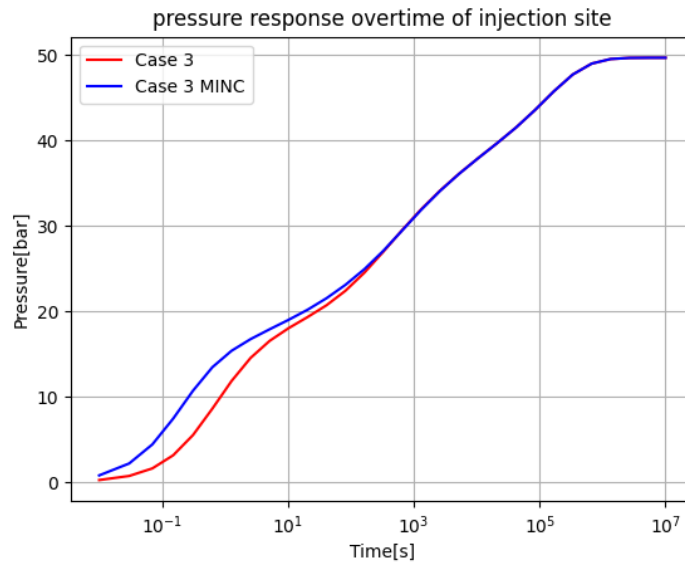


**Figure 3.4.3 Pressure profile of wavy case 3 at injection block.**

The pressure profile at injection block for case 4 of single porosity and MINC model shown in figure below.

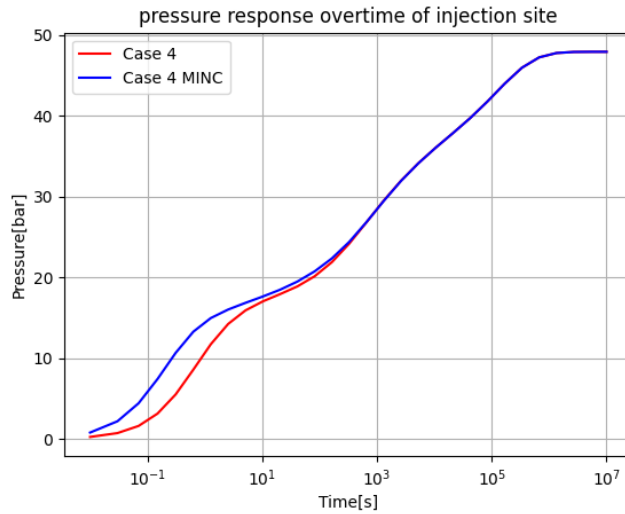


**Figure 3.4.4 Pressure profile of wavy case 4 at injection block.**

The pressure profile at injection block for case 5 of single porosity and MINC model shown in figure below.

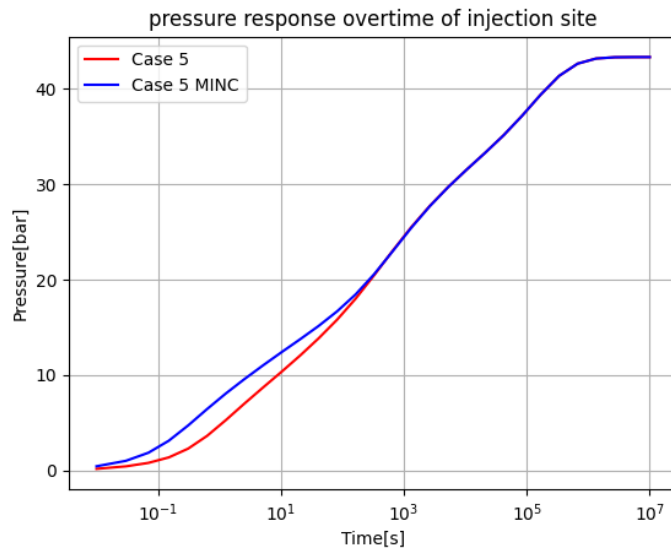


**Figure 3.4.5 Pressure profile of wavy case 5 at injection block.**

The pressure profile at injection block for case 6 of single porosity and MINC model shown in figure below.

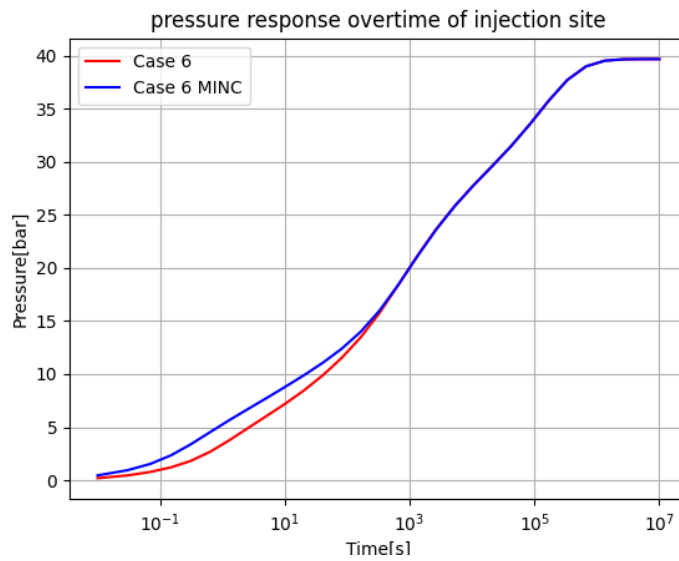


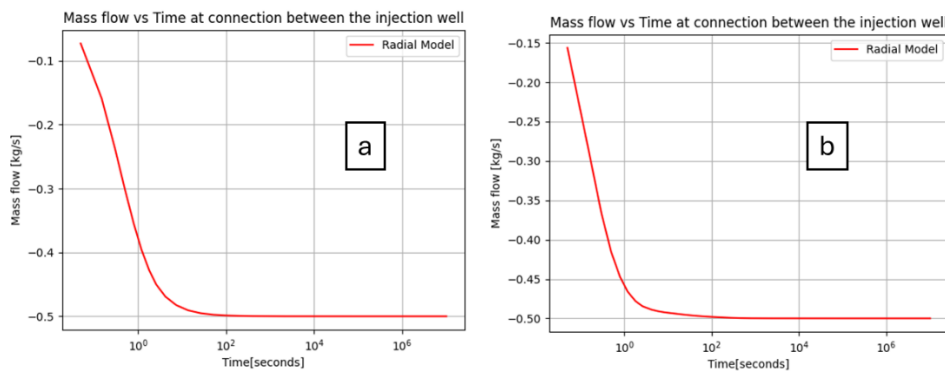
**Figure 3.4.6 Pressure profile of wavy case 6 at injection block.**

# Chapter 4

## Analysis and Discussion

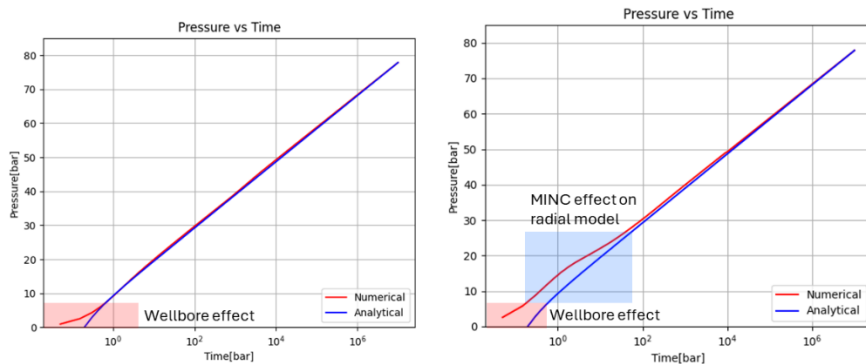
### 4.1 Radial Model

The comparison between the analytical model and numerical model has a difference in early timesteps. This is caused by the wellbore storage which could be explained by graphing the mass flow at the injection well and neighboring block as shown in the figure below.



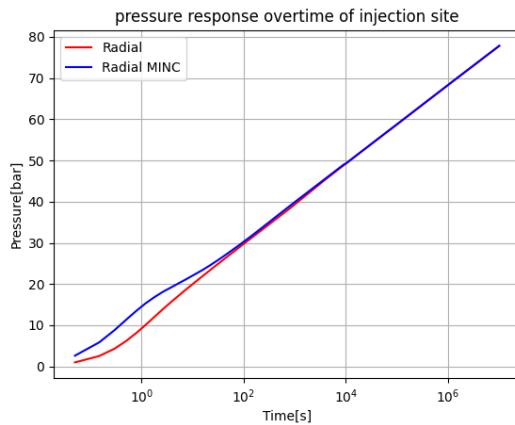
**Figure 4.1.1 Mass flow at injection well and neighboring block for non-MINC (a) and MINC (b) model**

In analytical model, there are two noticeable differences in non-MINC and MINC model. The first one which appeared on both models is the wellbore effect which happens at early timestep. The MINC model also shows a slight hump at first 100 seconds, this is common in MINC model because of the interaction between fracture and matrix.



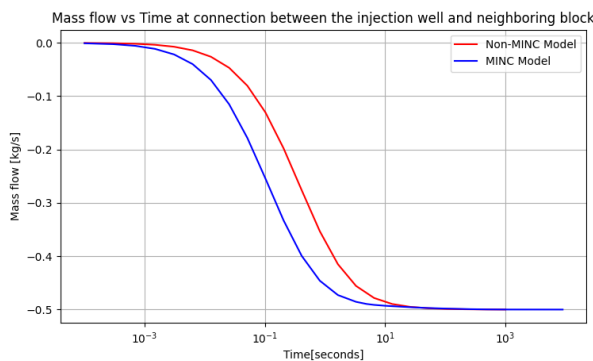
**Figure 4.1.2 Early wellbore effect at non-MINC (a) and MINC (b) model**

The comparison of the pressure profile between the non-MINC and MINC model, there is a major difference in early timestep shown in figure below.



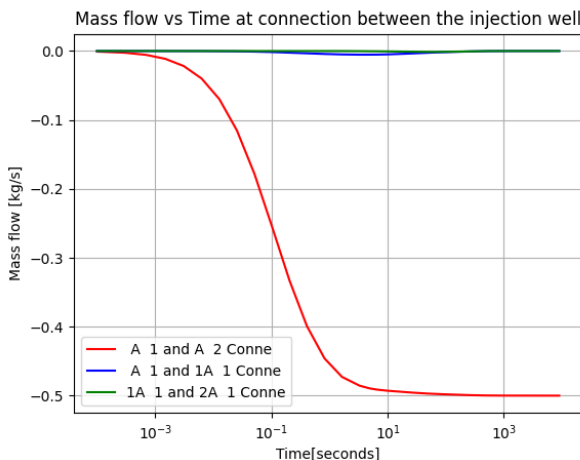
**Figure 4.1.3 Pressure profile of radial and radial MINC.**

This difference in wellbore storage period might be caused by the MINC model has faster response which shown in figure below.



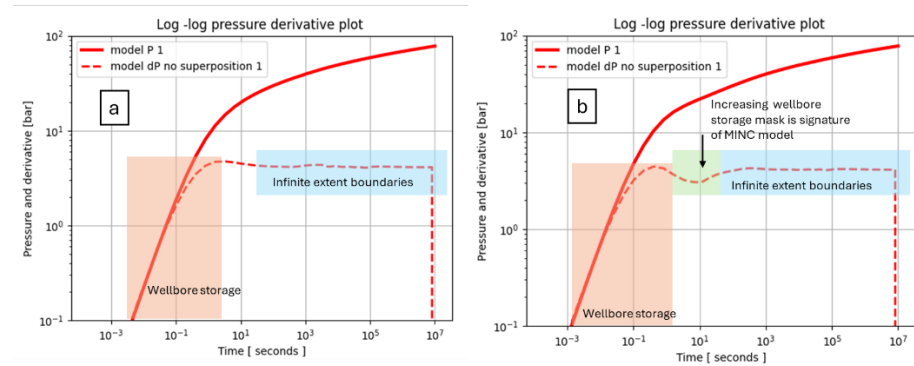
**Figure 4.1.4 Mass flow at connection between injection well and neighboring block in Non-MINC and MINC model.**

This is caused by the connection between the fracture and matrix block in MINC model that allows it to responds faster as shown in figure below.



**Figure 4.1.5 Mass flow of the Injection block for MINC Model**

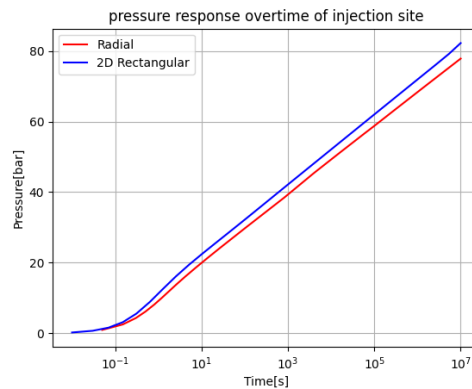
The pressure transient analysis result could be explained in the figure below.



**Figure 4.1.6 Pressure transient analysis for non-MINC (a) and MINC (b) Model**

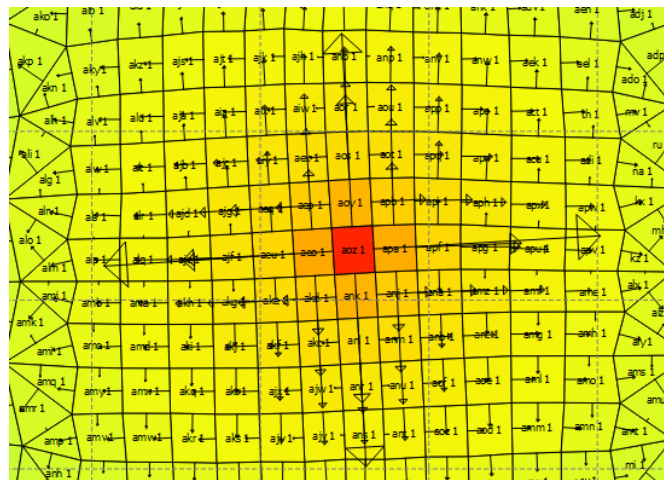
## 4.2 2D Rectangular Model

The comparison between the 2D rectangular and radial model is shown in figure below.



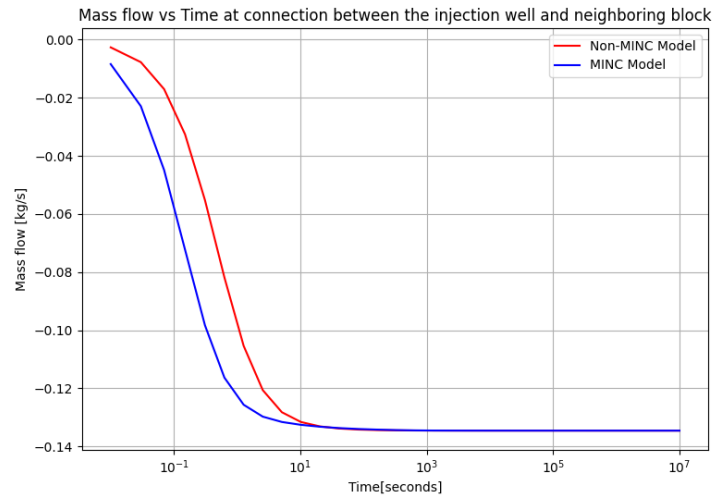
**Figure 4.2.1 Pressure profile of 2D rectangular and radial model at injection block**

This shows that the 2D rectangular model and radial model have similar pressure profile with slight differences in the pressure increase. This might be caused by the mass flow directions in 2D rectangular model that is more complex compared to radial model as shown in figure below.



**Figure 4.2.2 The mass flow direction of rectangular 2D model.**

As expected, the MINC model in 2D rectangular model affects the wellbore storage similarly to radial model as shown in mass flow with the neighboring blocks below.

**Figure 4.2.3 Mass flow comparison between the Non MINC and MINC model.**

### 4.3 3D Rectangular Model

The comparison between 3D rectangular model and 2D rectangular model at injection block shown in figure below.

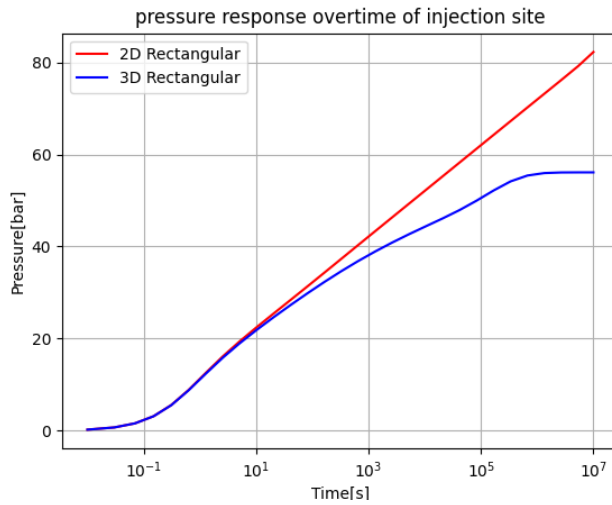


**Figure 4.3.1 The pressure profile at injection block of 2D and 3D Rectangular model.**

The result for the early timestep looks similar with a very different response after 10 seconds of Injection, this might be because in 2D rectangular model the top and bottom boundaries are closed where in 3D rectangular model there was still mass flow leaking into top and bottom boundaries even though it is relatively impermeable which could be shown in Figure 4.3.2.

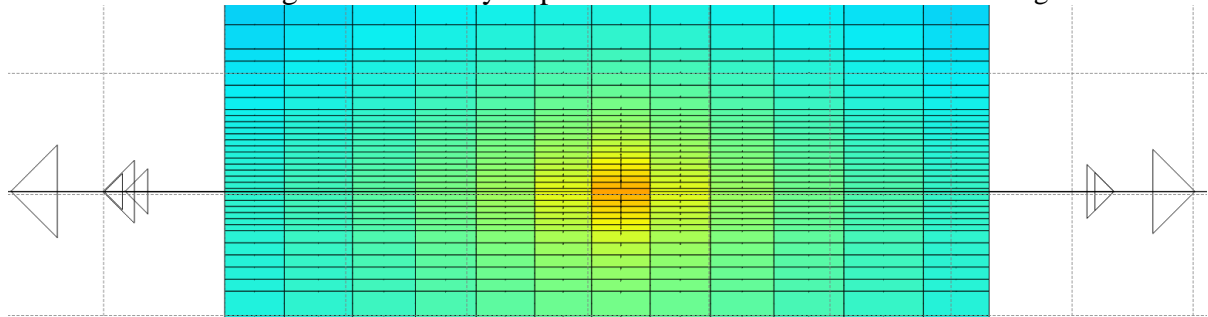


**Figure 4.3.2 Mass flow direction of the 3D rectangular model.**

Similarly with other models, the MINC model affects the wellbore which could be shown as the mass flow between injection block and neighboring block shown in Figure 4.3.3.

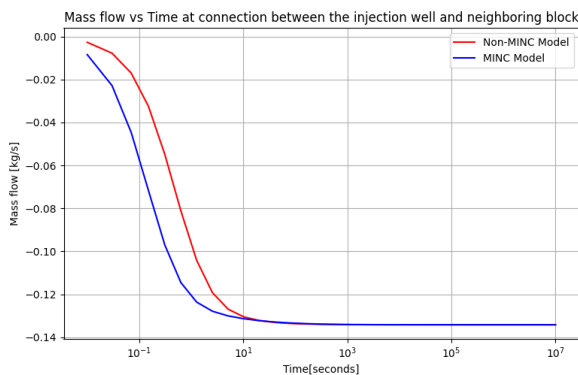


**Figure 4.3.3 The mass flow at injection block of 3D rectangular model.**

## 4.4 3D Rectangular Wavy Model

### 4.4.1 The amplitude impact on injection pressure

This section discusses how the amplitude of a wave impacted the injection pressure of an outcrop. The three figures below show that the model with one, two, and three wavelengths with different amplitude.

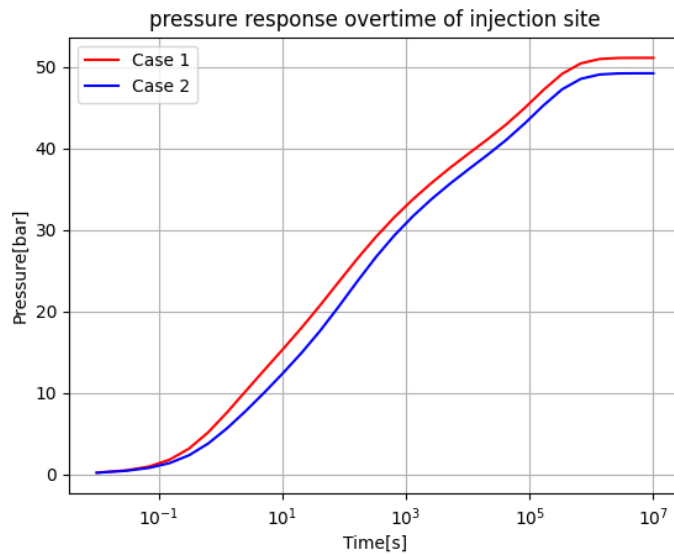


**Figure 4.4.1 Pressure profile at injection block for 1 wave.**

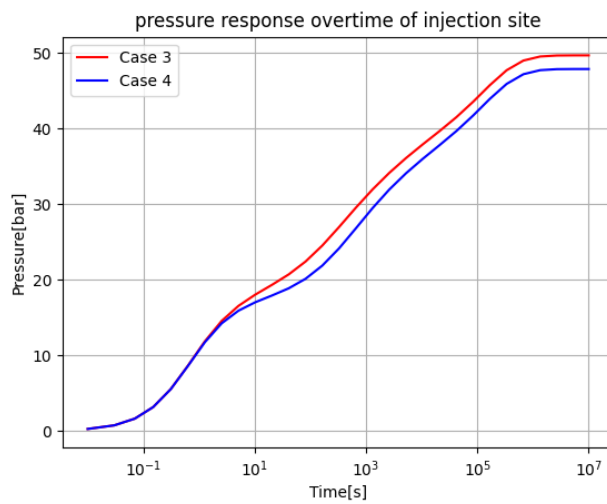


**Figure 4.4.2 Pressure profile at Injection block for 2 waves.**

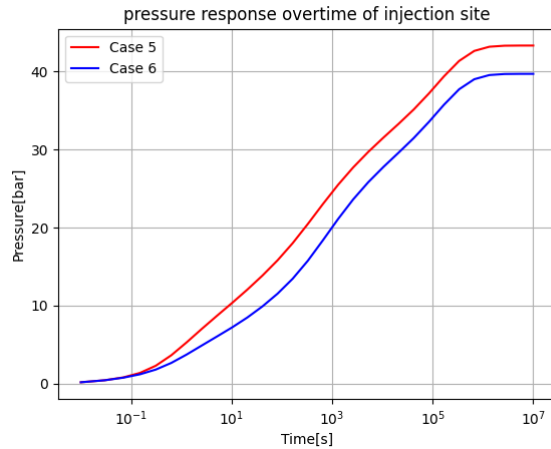


**Figure 4.4.3 Pressure profile at injection block for 3 waves.**

Based on three cases provided, we could determine that the larger amplitude lowers the injection pressure.

#### 4.4.2 Number of wave impact on injection pressure

This section discusses the effect of the amount of wave on the injection pressure. The figure below shows the pressure profile at injection block of three different number of waves for 2 different amplitudes.

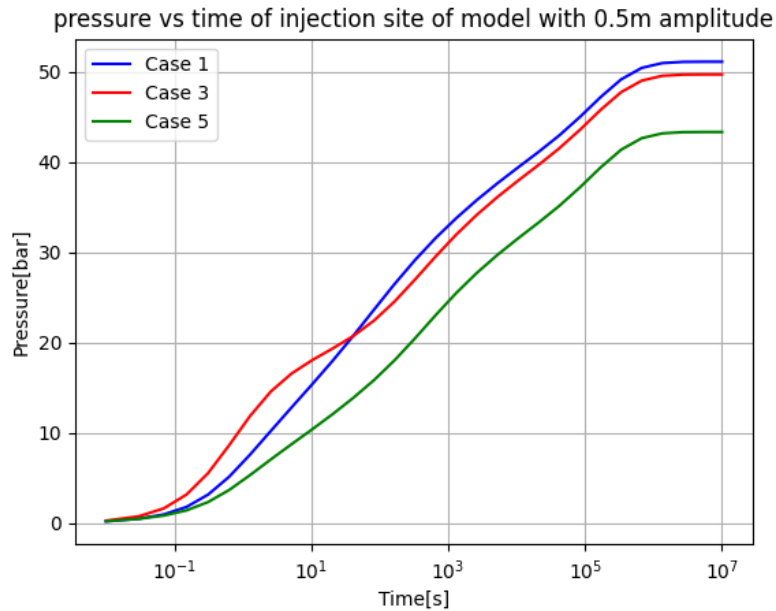


**Figure 4.4.4 Pressure profile at injection block of model with 0.5m amplitude.**

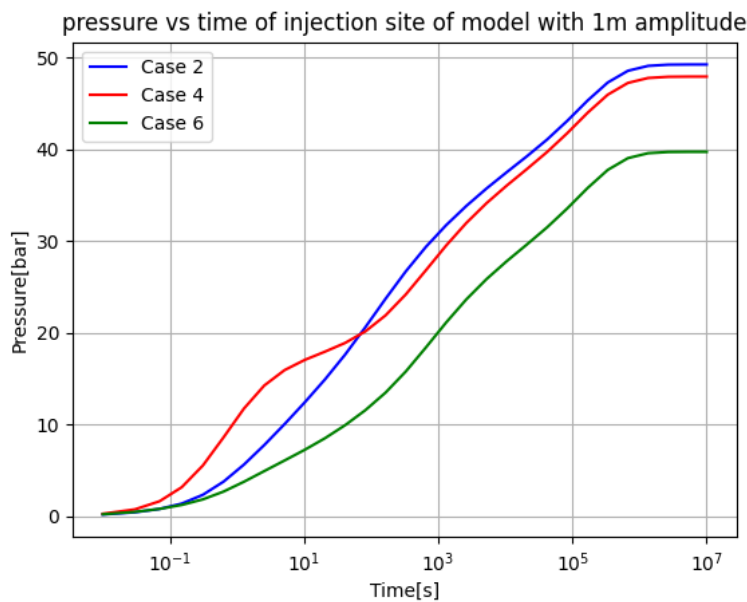


**Figure 4.4.5 Pressure profile at injection block of model with 1m amplitude.**

As shown in the two figures above, as the wave increased the pressure increase at injection block was lowered. However, this could not yet concluded before taking account of the mass flow and volume which will be discussed in the next section.

#### 4.4.3 The Volume impact on injection pressure

To match the volume of the blocks, the number of blocks was calculated which is shown in table below.

**Table 5 Number of blocks for every model**

Case	Block number
1	180
2	215
3	303
4	471
5	396
6	649

The graph containing the number of blocks effect on a model with case on flat model shown as below.

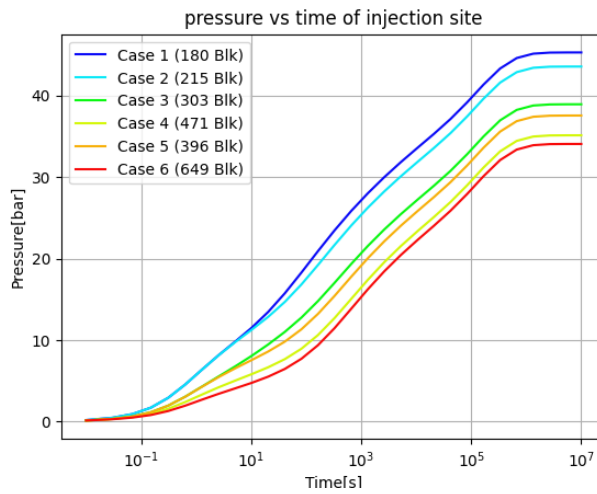


**Figure 4.4.6 Pressure profile at injection block for flat rectangular model with different volume.**

From the graph shown above, the more of the blocks lower the pressure profile in the injection block. With this observation, the data plotted comparing it to the model as shown in figure below.

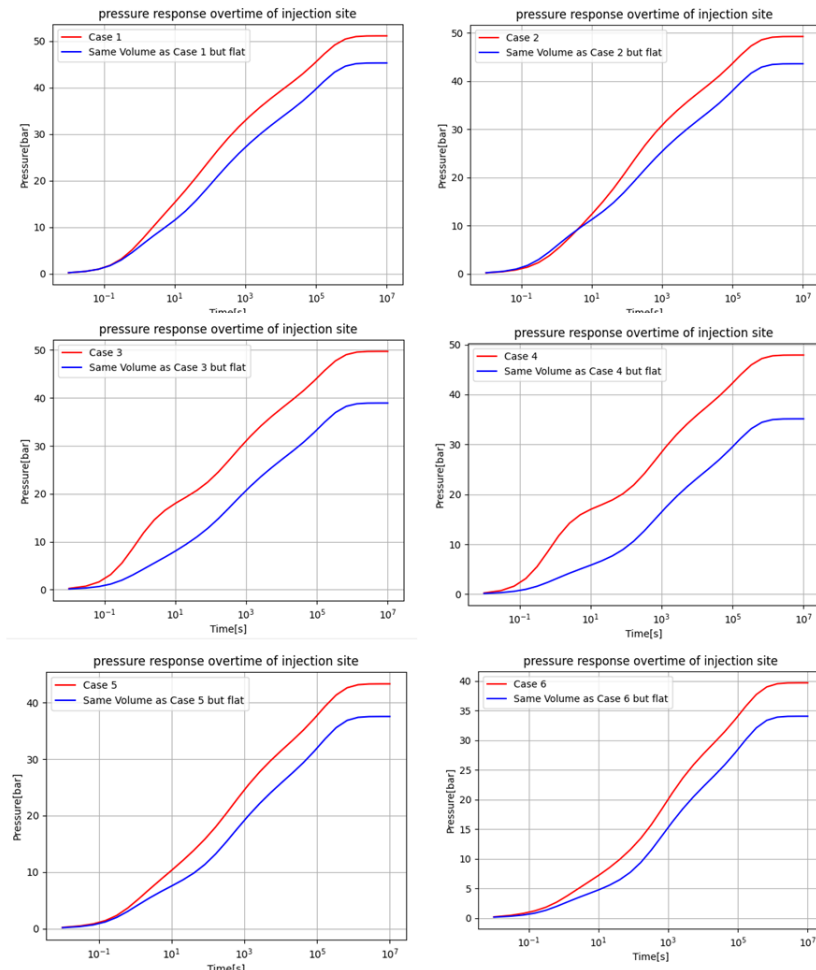


**Figure 4.4.7 The pressure profile of wavy model compared with the flat model with same number of blocks.**

This shows that the number of could also affect the pressure profile. However, there is no evidence that it is the primary properties that affect the pressure profile.

#### 4.4.4 Geometry effect on Mass flow direction

The mass flow direction of case 1 at injection block cross section shown below

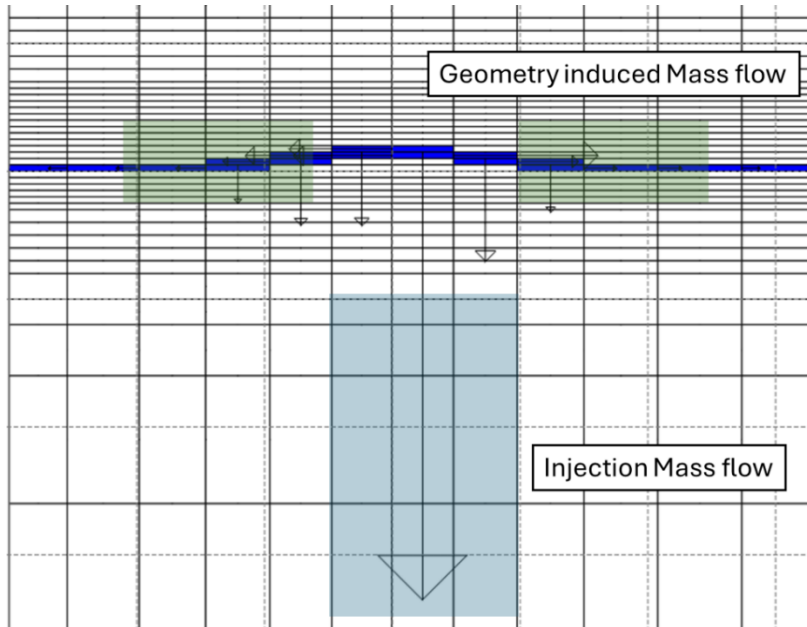


**Figure 4.4.8 Mass flow direction of Case 1 at Injection block cross section**

The mass flow direction of case 2 at injection block cross section shown below.

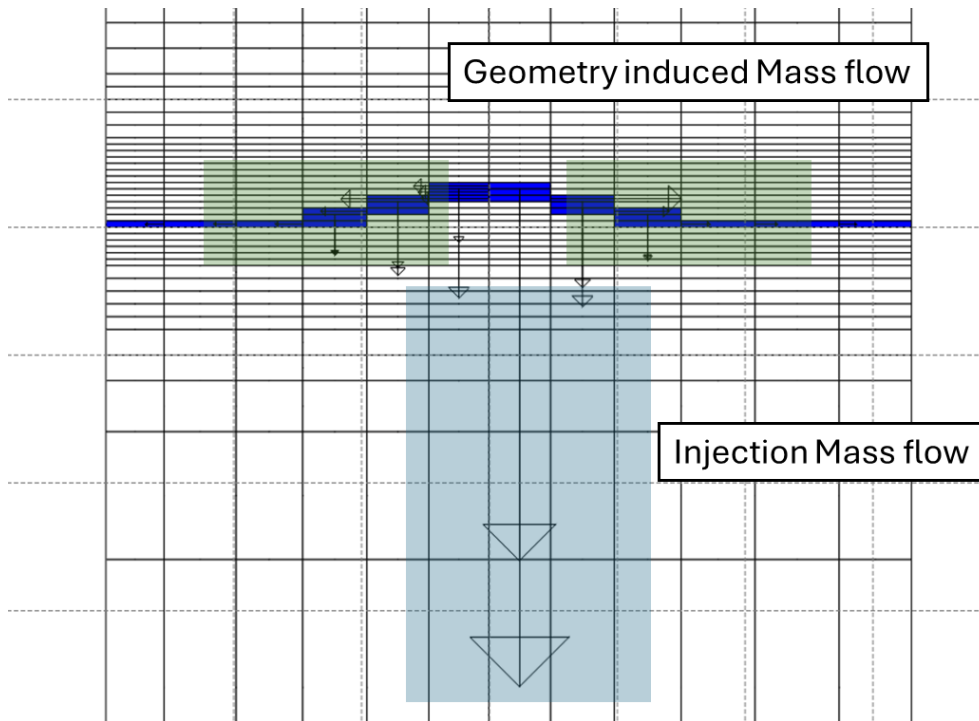


**Figure 4.4.9 Mass flow direction of Case 2 at Injection block cross section**

The mass flow direction of case 3 at injection block cross section shown below.

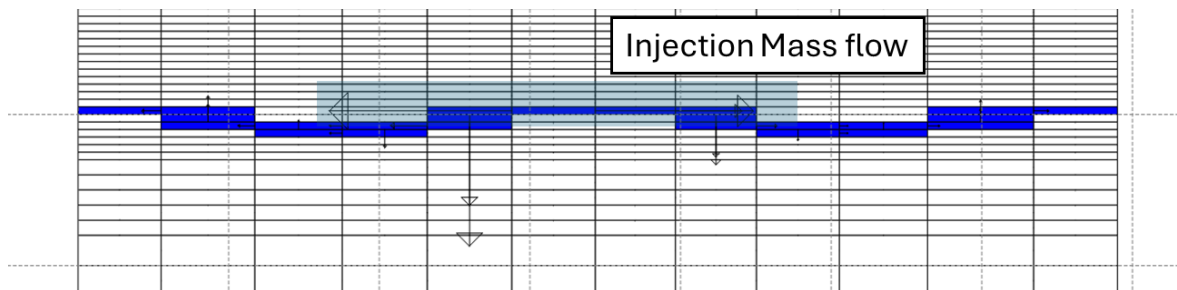


**Figure 4.4.10 Mass flow direction of Case 3 at Injection block cross section.**

The mass flow direction in the adjacent wave structure cross-section shows the movement pattern of the pressure follows the structure as shown below.

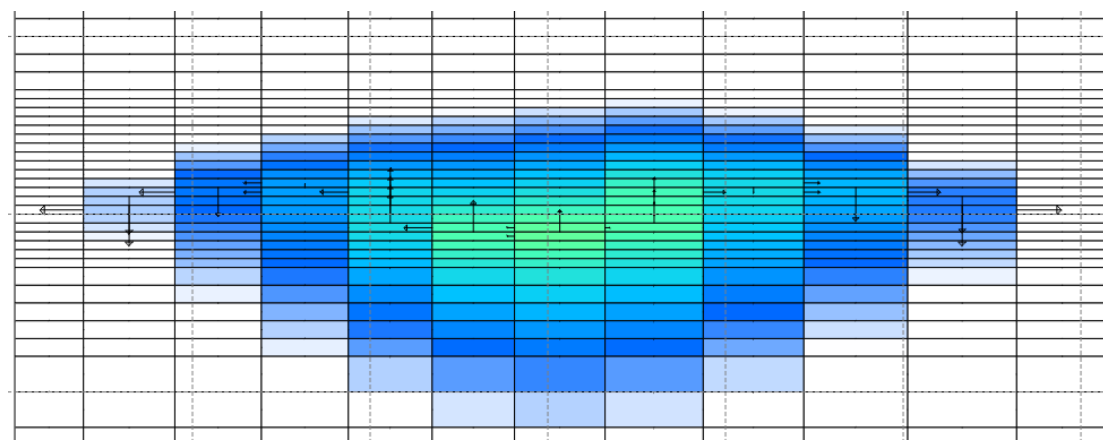


**Figure 4.4.11 Pressure cross section of the wave structure of Case 3.**

The mass flow direction of case 4 at injection block cross section shown below.

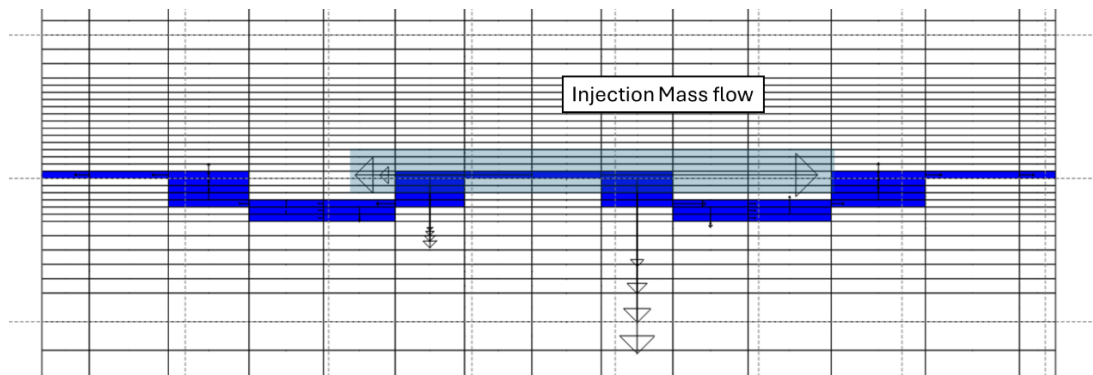


**Figure 4.4.12 Mass flow direction of Case 4 at Injection block cross section.**

Similar to Case 3, mass flow direction in the adjacent wave structure cross-section shows the movement pattern of the pressure follows the structure as shown below.

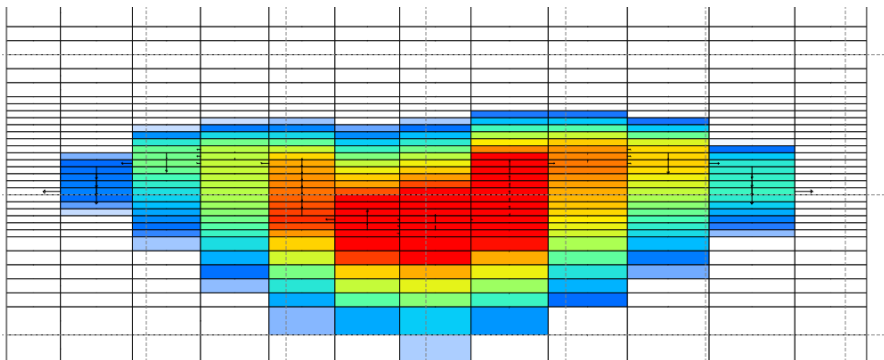


**Figure 4.4.13 Pressure cross section of the wave structure of Case 4.**

The mass flow direction of case 5 at injection block cross section shown below.

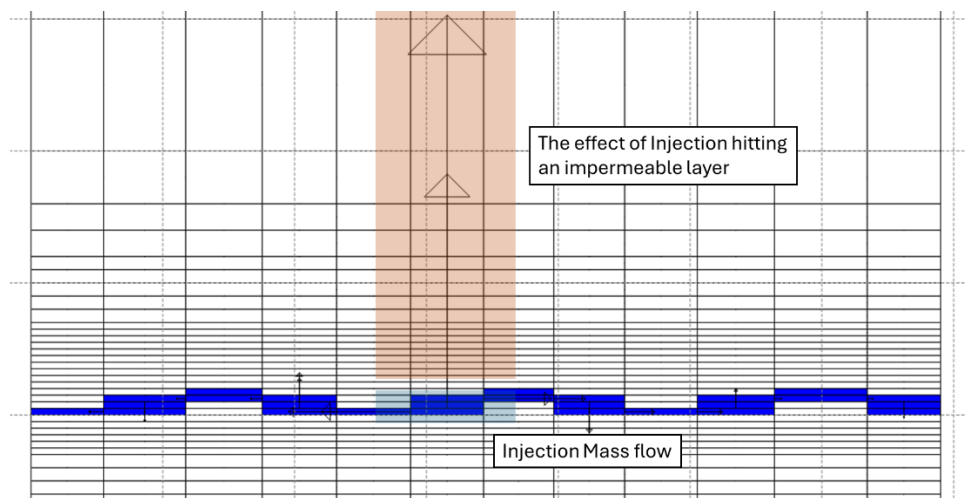


**Figure 4.4.14 Mass flow direction of Case 5 at Injection block cross section.**

Similarly to Case 3 and 4, mass flow direction in the adjacent wave structure cross-section shows the movement pattern of the pressure following the structure as shown below.

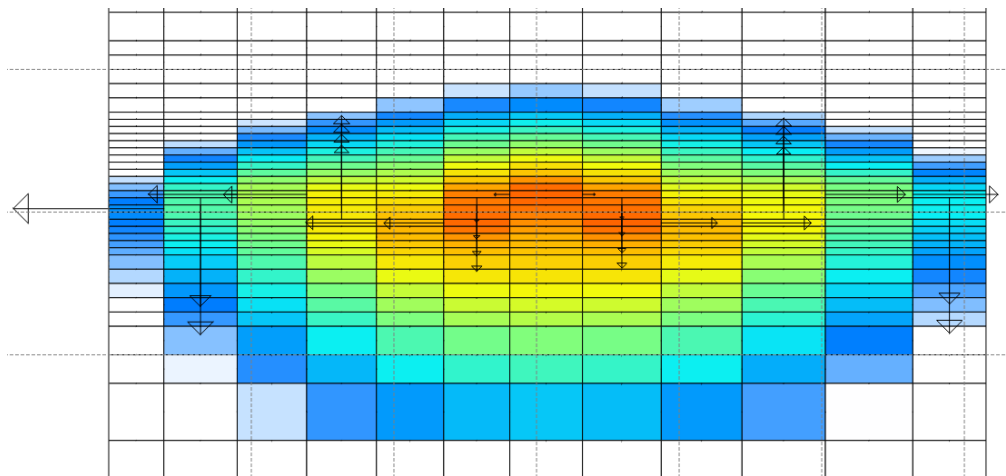


**Figure 4.4.15 Pressure cross section of the wave structure of Case 5.**

The mass flow direction of case 6 at injection block cross section shown below.

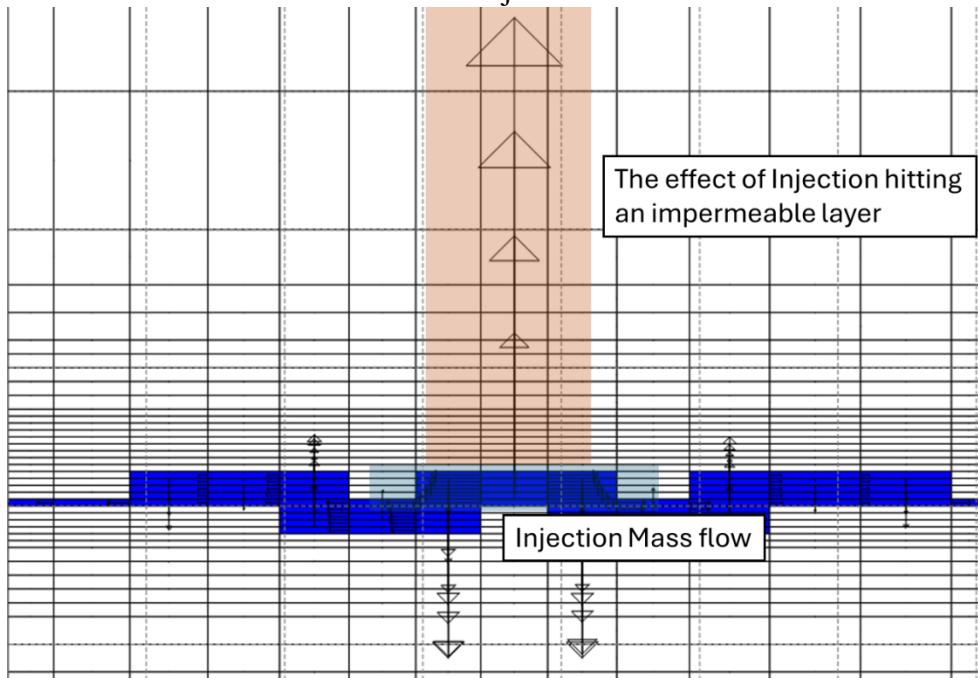


**Figure 4.4.16 Mass flow direction of Case 6 at Injection block cross section.**

Similarly to Case 3, 4, and 5, mass flow direction in the adjacent wave structure cross-section shows the movement pattern of the pressure following the structure as shown below.

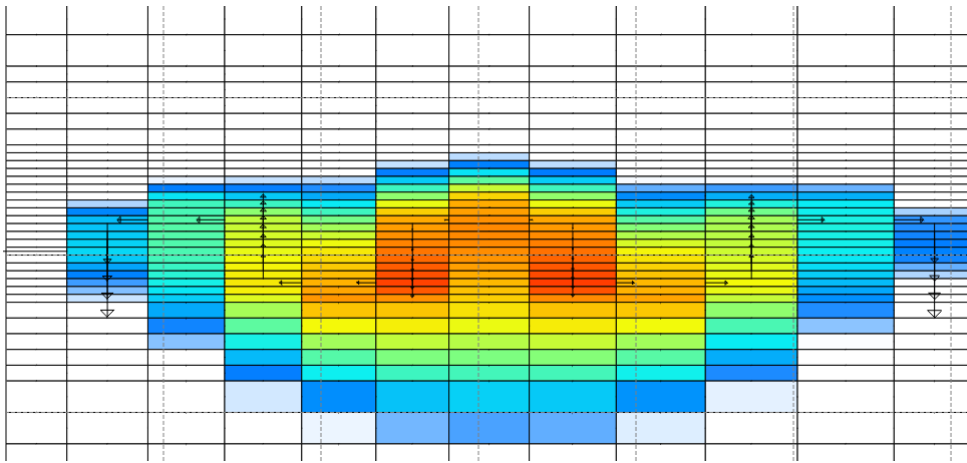


**Figure 4.4.17 Pressure cross section of the wave structure of Case 6**

Based on the observations of the mass flow directions of 6 different wave models, the pressure profiles of the model seem to be affected by the model.

From Case number 5 and 6 above, the mass flow seems to be going upwards after injection, further investigation conducted on this model to determine whether this affects the entire model shown in figure below.



**Figure 4.4.18 Modified Case 5 and 6 cross section with mass flow arrow.**

Using this model, the model compared with the initial model which shown in figure below

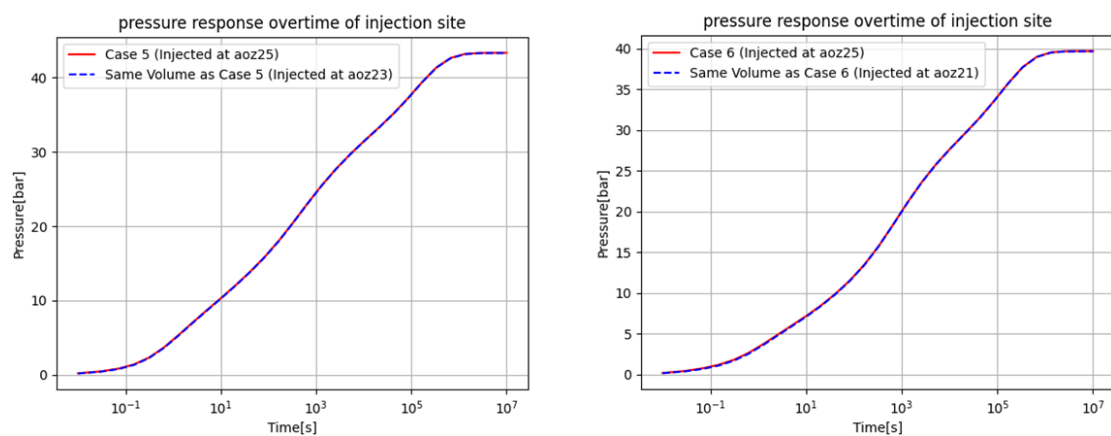


**Figure 4.4.19 Comparision between the initial and modified Case 5 and 6**

According to this observation, the injection depth does not affect the model at all.

# Chapter 5

## Conclusion and Future Works

### 5.1 Conclusion

The research successfully investigated the different geometry effects found in Northern Reykjanes Peninsula on injection pressure using AUTOUGH2. This also includes providing workflow to investigate the different geometry that could be found in permeability zones and sequence of basaltic flow. The conclusion of this investigation is that the wavy surface does affect the isothermal injection of the freshwater interface. Specifically:

- The larger the amount of amplitude, the lower the injection pressure.
- The more waves appeared on the model, the lower the injection pressure.
- The volume of the model affected the model.
- The geometry heavily influenced the injection pressure results.

Moreover, the workflow for this research has been executed successfully starting from validating the radial model result with analytical methods and pressure transient, comparing the results of the 2D rectangular model with the radial model, and building more complexity of the 3D rectangular model.

### 5.2 Future Work

The research has so much potential for continuation especially since the plan of using drone to measure the real geometry of the outcrop was cancelled. The data from the drone measurement could provide more complexity to the model by adding more layers of rock that represents the actual outcrop. The other thing that could be added into the research includes adding the salt-water interface and geochemistry measurement to the reservoir simulation.

# Appendix A: Code

## A.1. Code for MINC making.

mincmaker.py

```

1. from t2data import*
2.
3. #import .dat file
4. dat = t2data('file.dat')
5.
6. #Specify the parameters
7. vol_fraction = [0.3,0.3,0.4]
8. spacing = 10
9. num_fracture_planes = 2
10. #block input could also be efficiently inputted using TIM
11. blocks = dat.grid.blocklist[:-1]
12. matrix_blockname = None
13. minc_rockname = None
14. proximity = None
15. #atmos_vol must be specified to determine the volume of blocks that included in boundary
16. #conditions
17. atmos_vol = 3.3e0
18. #INCON could be included if needed
19. incon = None
20. fracture_connection_distance = 0.3
21.
22. dat.grid.minc(vol_fraction,spacing,num_fracture_planes,blocks,matrix_blockname,minc_rock\
23. name,proximity,atmos_vol,incon,fracture_connection_distance)
24. #write the MINC dat file
25. dat.write('fileMINC.dat')
```

## A.2. Script for Refining Geometry

**Required file:** .dat file containing the x-axis and y-axis of the polygon. This could easily be obtained using TIM.

```
1. #Import the required script
2. from t2grids import *
3. import numpy as np
4.
5. #Import the geometry
6. geo=mulgrid('non_refinedgrid.dat')
7. #Import the polygon that wants to be refined
8. columns_refine=np.loadtxt('polygon.dat',delimiter=',')
9. #Optionally you can print this to make sure it is the right blocks to refine
10. print(columns_refine)
11. #finds the skinny columns to refined
12. skinny_columns=geo.columns_in_polygon(columns_refine)
13. print (skinny_columns)
14. geo.refine(skinny_columns)
15. geo.write('refinedgrid.dat')
```

## A.3. Script for optimize the Geometry

**Required file:** .dat file containing the x-axis and y-axis of the polygon. This could easily be obtained using TIM.

```
1. #Import the required script
2. from t2grids import *
3. import numpy as np
4.
5. #Import the geometry
6. geo=mulgrid('non_optimizedgrid.dat')
7. #Import the polygon that wants to be optimized
8. opt = np.loadtxt('polygon.dat',delimiter=',')
9. opt_nodes = geo.nodes_in_polygon(opt)
10. #Optionally you can print to make sure you get the right block to optimized
11. print(opt_nodes)
12.
13. #Script for optimizing the grids
14. opt_nodes_list=[tempnode.name for tempnode in opt_nodes]
15. geo.optimize(opt_nodes_list, 1.0, 0.5, 0.0, False)
16. geo.write('optimizedgrid.dat')
```

## A.4. Code for Generating Radial Model

The script to create radial model shown below:

*radial\_maker.py*

```

1. from t2data import *
2. from math import log10, log, pi, gamma, exp
3.
4. #Default parameters for Infinite extent radial model
5. skin_zone_radius = 5.0
6. model_extent = 20000.0
7. num_skin_blocks = 50
8. num_res_blocks = 100
9.
10. #Parameters needed for the model
11. well_radius = 1.12 #in meter
12. layer_thickness = 0.25 #Meters of reservoirs
13. well_volume = 1.6786 #units m3
14.
15. #Calculate the grid bloc
16. res_k_estimate = 5.0e-13 #reservoir permeability
17. sf = -2.0 #skin factor
18. n = 2.0
19. ks = res_k_estimate/(1+(sf/log(skin_zone_radius/well_radius)))
20. kskin = [ks]*3
21.
22. #Define array for vertical thickness
23. dz = np.array([layer_thickness])
24. orig = np.array([0.,0.,-342.0])
25. #Create log spaced block radii in skin zone and reservoir zone (do not touch this)
26. skin_blk = np.logspace(log10(well_radius), log10(skin_zone_radius), num\
27. num_skin_blocks)
28. res_blk = np.logspace(log10(skin_zone_radius), log10(model_extent), num =\
29. num_res_blocks + 1)
30.
31. #Create delta radius / dr
32. dr = [0.0]
33. dr[0] = well_radius
34. for i in range(1, len(skin_blk)):
35.     x = skin_blk[i] - skin_blk[i-1]
36.     dr.append(x)
37. for i in range(1, len(res_blk)):
38.     x = res_blk[i] - res_blk[i-1]
39.     dr.append(x)
40. #Fractional Dimension Calculation (Do not touch this)
41. all_blk_radii =[0.0]
42. all_blk_radii[0] = well_radius
43.
44. for i in range(1, len(dr)):
45.     x = all_blk_radii[i-1] + dr[i]
```

```

46.    all_blk_radii.append(x)
47.
48. #use radii to calculate original volumes
49. original_volumes = [0.0]
50. x = pi*layer_thickness*all_blk_radii[0]**2
51. original_volumes[0] = x
52.
53. for i in range(1, len(all_blk_radii)):
54.     x = pi*layer_thickness*(all_blk_radii[i]**2 - all_blk_radii[i-1]**2)
55.     original_volumes.append(x)
56.
57. #use radii to calculate original connection areas
58. original_conneareas = [0.0]
59. x = 2*pi*all_blk_radii[0]*layer_thickness
60. original_conneareas[0] = x
61.
62. for i in range (1, len(all_blk_radii)):
63.     x=2*pi*all_blk_radii[i]*layer_thickness
64.     original_conneareas.append(x)
65.
66. #Calculation of fractional dimension required in order to make the first connection area equal
67. #to the original area
68. first_connection = original_conneareas[0]
69. alpha_n = (2*(pi**((n/2)))/gamma(n/2))
70. b = exp((1/(3-n))*log(first_connection/(alpha_n*all_blk_radii[0]**(n-1))))
71.
72. #Use radii to calculate FD Volumes
73. FD_vols = [0.0]
74.
75. for i in range(1, len(all_blk_radii)):
76.     x = ((alpha_n*(b**((3-n))/n)*(all_blk_radii[i]**(n-1)-all_blk_radii[i-1]**(n-1)))
77.     FD_vols.append(x)
78.
79. #Use radii to calculate FD connection areas
80. FD_conneareas = [0.0]
81. x = alpha_n*(b**((3-n))*(all_blk_radii[0]**(n-1))
82. FD_conneareas[0] = x
83.
84. for i in range(1, len(all_blk_radii)):
85.     x = alpha_n*(b**((3-n))*(all_blk_radii[i]**(n-1))
86.     FD_conneareas.append(x)
87. #Create t2 dat file
88. dat = t2data()
89. dat.title = 'Radial Model'
90. dat.simulator = 'AUTOUGH2.2W'
91. dat.multi = {'eos': 'EW', 'num_components': 1, 'num_equations': 1, 'num_phases': 2, /
92. 'num_secondary_parameters': 6}
93. dat.start = True
94. #RPCAP
95. dat.relative_permeability = {'parameters': [0.5,0.0,1.0,0.5,0.0], 'type' : 1}
96. dat.capillarity = {'parameters': [0.0,0.0,1.0,0.0,0.0], 'type' : 1}
97. #Grid creation

```

```

98. dat.grid = t2grid().radial(dr, dz, convention = 2, origin = orig, case = 'A')
99.
100. for blk in dat.grid.blocklist:
101.     i = int(blk.name[2:5])
102.     x = FD_vols[i-1]
103.     blk_volume = x
104.
105. for conn in dat.grid.connectionlist:
106.     i = int(conn.block[0].name[2:5])
107.     x = FD_conneareas[i-1]
108.     conn.area = x
109.
110. dat.grid.delete_rocktype('dfalt')
111. #Add rocktype
112. r1 = rocktype(name= 'RESER', permeability= [10.e-15]*3)
113. dat.grid.add_rocktype(r1)
114. for blk in dat.grid.blocklist[0:]:
115.     blk.rocktype = dat.grid.rocktype['RESER']
116. dat.parameter['default_incons'] = [initial_reservoir_pressure*1.e05,/
117. initial_reservoir_temperature]
118. #add_generation
119. gen = t2generator(name = 'wel 1', block = dat.grid.blocklist[0].name,
120.                     type= 'MASS ',
121.                     rate = 0.5
122.
123. dat.add_generator(gen)
124. dat.write('radial.dat')

```

This script does not include the controlled timestep. It is recommended to input the controlled timestep using notepad application since it is more likely to encounter an unnecessary struggle. The example of controlled timestep shown below which located in PARAM section of the tough2 script.

```

.....
PARAM
0 3 999 0 99910000010022000500000010 0.000e+00 0.000e+00
0.000e+00 1.000e+07-6.000e+00 1.140e+04 A 1 9.8100e+00
1.0000e-031.0000e-011.5000e-012.0000e-013.0000e-014.0000e-016.0000e-018.0000e-01
4.8000e+001.2000e+014.8000e+019.6000e+011.2000e+022.4000e+024.8000e+024.8000e+02
4.8000e+024.8000e+024.8000e+024.8000e+024.8000e+024.8000e+024.8000e+024.8000e+02
9.6000e+029.6000e+029.6000e+029.6000e+029.6000e+029.6000e+029.6000e+029.6000e+02
1.9200e+031.9200e+031.9200e+031.9200e+031.9200e+031.9200e+031.9200e+031.9200e+03
3.8400e+033.8400e+033.8400e+033.8400e+033.8400e+033.8400e+033.8400e+033.8400e+06
.....

```

## A.5. Code for converting .LISTING to CSV

lst\_csv.py

```

1. from t2listing import*
2. import numpy as np
3.
4.
5. lst = t2listing('file.listing')
6. time, press = lst.history(('e','[[NAME OF BLOCKS]]','Pressure'))
7. press_bar = press/100000
8.
9. #Save text to csv files
10. np.savetxt('file.csv', np.vstack((time, press_bar)).T, delimiter=',')

```

## A.6. Code to plot semilog graph

semilogplot.py

```

1. import numpy as np
2. import matplotlib.pyplot as plt
3.
4. #Input the required parameters
5. press1 = np.loadtxt('file1.csv', delimiter=',')
6. press1_time = np.array(list(press1[:,0]))
7. press1_P = np.array(list(press1[:,1]))
8.
9. plt.semilogx(press1_time, press1_P, color='red', label='[[proper_label]])')
10. plt.legend(loc='best')
11. plt.grid(True)
12. plt.title('pressure vs time of injection site')
13. plt.xlabel('Time[s]')
14. plt.ylabel('Pressure[bar]')
15. plt.show()

```

## A.7. Pressure Transient Analysis

The pressure transient analysis python script created with the assistance of the previous thesis dissertation by (McLean, 2020).

### Required file for PT

# Flowdata file

The file specifies the time and mass flow, for one step pressure transient only two timestep required which is the starting timestep and when the transient finished. The example is shown below.

```
Flow_datafile.csv
#time in seconds, mass flow in kg/s#
0, 0.5
107,0.5
```

# Conversion of .listing file to csv explained in **Appendix A.3.**  
pressure\_transient.py

```
1. #import necessary library
2. from t2listing import*
3. import numpy as np
4. import matplotlib.pyplot as plt
5. from math import log10, log
6.
7. #Import csv file from previous step
8. press1 =np.loadtxt('file1.csv', delimiter=',')
9. press1_time = np.array(list(press1[:,0]))
10. press1_P= np.array(list(press1[:,1]))
11.
12. #Import flow data file
13. FLOW = np.loadtxt('flow_datafile.csv', delimiter=',')
14. FLOW_time = np.array(list(FLOW[:,0]))
15. FLOW_rate = np.array(list(FLOW[:,1]))
16.
17. ##Calculation derived from (McLean, 2020)##
18. ##Define function for superposition time and derivative calculations##
19.
20. diff_int = 0.2
21. def calculate_superposition_time(array_time, array_flowtimes, array_flowrate):
22.     if not len(array_flowrate)==len(array_flowtimes):
23.         sys.exit("arrays not same length")
24.     sup_t = np.empty(len(array_time),dtype=float)
25.     N = len(array_flowrate)
26.     q = array_flowrate
27.     t = array_flowtimes
28.
29.     for x in range(0,len(array_time)):
```

```

30.     sup_t[x] = log10(array_time[x])
31.
32.     for i in range(0,N-1):
33.         if i==0:
34.             temp = (q[i]/(q[N-1]-q[N-2]))*log10(t[N-1]-t[i]+array_time[x])
35.             sup_t[x] = sup_t[x] + temp
36.         else:
37.             temp = ((q[i]-q[i -1]) /(q[N -1] - q[N -2])) * log10 (t[N -1] -t[i]+array_time[x])
38.             sup_t[x] = sup_t[x] + temp
39.     return sup_t
40.
41. def calculate_delta ( array_data ):
42.     delta = np.empty(len(array_data) - 1, dtype=float)
43.
44.     for i in range (0, len( delta )):
45.         temp = array_data[i + 1] - array_data[0]
46.         delta[i] = abs(temp)
47.     return delta
48.
49. def find_ln_sep_points(array, i, interval):
50.     j = 1
51.     k = 1
52.     while i + j <= len(array) - 1:
53.         if i == 0:
54.             break
55.         if log(array[i + j]) - log(array[i]) >= interval:
56.             break
57.         if log( array [i+j]) - log( array [i]) < interval and i+j == len( array ) -1:
58.             j = 0
59.             break
60.         j = j + 1
61.     if i == len(array) - 1:
62.         j = 0
63.
64.     while i-k > 0:
65.         if log(array[i]) - log(array[i - k]) >= interval:
66.             break
67.         if log(array[i]) - log(array[i - k]) < interval and i - k == 0:
68.             k = 0
69.             break
70.         k = k + 1
71.
72.     if i == 0 or i == 1:
73.         k = 0
74.
75.     return j, k
76.
77. #Function to calculate smooth derivative
78. def calculate_smooth_derivative ( array_time ,ar_dP ,ar_Sn , diff_interval ):
79.     deriv_smooth = np.empty(len(array_time), dtype=float)
80.     j_indices = np.empty(len(array_time), dtype=int)
81.     k_indices = np.empty(len(array_time), dtype=int)

```

```

82.
83.     for i in range(0, len(array_time)):
84.         j, k = find_ln_sep_points(array_time, i, diff_interval)
85.         j_indices[i] = j
86.         k_indices[i] = k
87.
88.     for i in range (0, len( array_time )):
89.         if i==0:
90.             deriv_smooth[i] = 0.0
91.         else:
92.             j = j_indices[i]
93.             k = k_indices[i]
94.             if j == 0 or k == 0:
95.                 deriv_smooth[i] = 0.0
96.                 continue
97.             if i-k<0 or i+j>len( deriv_smooth ):
98.                 deriv_smooth[i] = -9999.0
99.                 continue
100.
101.            temp = ar_dP[i + j] * ((ar_Sn[i] - ar_Sn[i - k]) / ((ar_Sn[i + j] - ar_Sn[i]) *\ 
102.                               (ar_Sn[i+j] - ar_Sn[i-k]))) + ar_dP[i]*((ar_Sn[i+j] + ar_Sn[i-k]-2 * ar_Sn[i]) /\ 
103.                               ((ar_Sn[i+j] - ar_Sn[i]) * (ar_Sn[i+j] - ar_Sn[i-k]))) - ar_dP[i-k]*((ar_Sn[i+j]-\ 
104.                               ar_Sn[i])/(( ar_Sn [i]- ar_Sn [i-k] * ( ar_Sn [i+j] - ar_Sn [i-k]))))
105.            deriv_smooth[i] = temp / 2.303
106.    return deriv_smooth
107. def calculate_smooth_derivative_noSn (ar_t,ar_dP , diff_interval ):
108.     deriv_smooth_bad = np.empty(len(ar_t), dtype=float)
109.     j_indices = np.empty(len(ar_t), dtype=int)
110.     k_indices = np.empty(len(ar_t), dtype=int)
111.
112.     ln_t_2 = calculate_ln_time(ar_t)
113.
114.     for i in range(0, len(ar_t)):
115.         j, k = find_ln_sep_points(ar_t, i, diff_interval)
116.         j_indices[i] = j
117.         k_indices[i] = k
118.
119.     for i in range(0, len(ar_t)):
120.         if i == 0:
121.             deriv_smooth_bad[i] = 0.0
122.         else:
123.             j = j_indices[i]
124.             k = k_indices[i]
125.             if j == 0 or k == 0:
126.                 deriv_smooth_bad[i] = 0.0
127.                 continue
128.             if i - k < 0 or i + j > len(deriv_smooth_bad):
129.                 deriv_smooth_bad[i] = -9999.0
130.                 continue
131.
132.             temp = ar_dP[i + j] * ((ln_t_2[i] - ln_t_2[i - k]) / ((ln_t_2[i + j] - ln_t_2[i]) *( ln_t_2\
133.                               [i+j]- ln_t_2 [i-k]))) + ar_dP[i] * ((ln_t_2[i + j] + ln_t_2 [i-k]-2* ln_t_2 [i]) /(( ln_t_2\
```

```

134.      [i+j]- ln_t_2[i]) * (ln_t_2[i]- ln_t_2[i-k])) - ar_dP[i-k] * ((ln_t_2[i+j]- ln_t_2[i]) \A
135.      ((ln_t_2[i]-ln_t_2[i-k]) * (ln_t_2[i+j]- ln_t_2[i-k])))
136.      deriv_smooth_bad[i] = temp
137.      return deriv_smooth_bad
138. def calculate_ln_time(array_time):
139.     array_ln_time = np.empty(len(array_time), dtype=float)
140.
141.     for i in range(0, len(array_time)):
142.         temp = np.log(array_time[i])
143.         array_ln_time[i] = temp
144.
145.     return array_ln_time
146. #calculating delta
147. delta_time_1 = calculate_delta(press1_time)
148. delta_P_1 = calculate_delta(press1_P)
149. #Specify the flow steps
150. temp_FLOW_time = FLOW_time[: 0]
151. temp_FLOW_rate = FLOW_rate[: 0]
152. #calculating superposition time
153. Sn_1 = calculate_superposition_time(delta_time_1,temp_FLOW_time,temp_FLOW_rate )
154. ln_time_1 = calculate_ln_time(delta_time_1)
155.
156. #calculate derivatives with and without superposition time
157. smooth_deriv_1 = calculate_smooth_derivative(delta_time_1, delta_P_1, Sn_1, diff_int)
158. smooth_deriv_no_superposition_1 = calculate_smooth_derivative_noSn(delta_time_1,\
159. delta_P_1, diff_int)
160. np.savetxt ('model_superposition_time_and_deriv_1.csv', np.vstack ((delta_time_1\
161. ,delta_P_1,Sn_1 ,smooth_deriv_1 ,smooth_deriv_no_superposition_1)).T\
162. ,delimiter=',', header='delta time (s), delta pressure (bar), Superposition time , smooth dP (bar),\\
163. smooth dP no Sn(bar)') #plot derivative
164. delta_time_1_crop = delta_time_1[:-1]
165. delta_P_1_crop = delta_P_1[:-1]
166. smooth_deriv_1_crop = smooth_deriv_1[:-1]
167. smooth_deriv_no_superposition_1_crop = smooth_deriv_no_superposition_1[:-1]
168.
169. #####PLOT EVERYTHING#####
170. plt.plot(delta_time_1_crop, delta_P_1_crop, color='red', label='model P 1')
171. #plt.plot(delta_time_1_crop, smooth_deriv_1_crop,'r-',linewidth=2.0 ,label ='model dP 1')
172. plt.plot(delta_time_1_crop, smooth_deriv_no_superposition_1_crop, color='red', label='model\
173. dP no superposition 1')
174. plt.xscale("log")
175. plt.yscale("log")
176. #plt.xlim(0.1,1000000)
177. plt.ylim(0.1,100)
178. plt.xlabel('Time [ seconds ]')
179. plt.ylabel('Pressure and derivative [bar]')
180. plt.grid(True)
181. plt.legend(loc='upper left', fontsize=10)
182. plt.title('Log -log pressure derivative plot ')
183. plt.savefig('model_superposition_time_and_deriv_1.png')
184. plt.show()

```

## A.8. Modern Theis Analytical Solution

### Required Files for the script.

#Flow data files required in the script, this includes the time in first column followed by mass flow in second column. In this file, the more data provided means the more details added in calculation. This could easily be generated using excel.

Example shown below.

Flowrate.csv

```
time,flowrate
8.00E-02,-5.00E-01
9.00E-02,-5.00E-01
1.00E-01,-5.00E-01
...
...
...
7.00E+06,-5.00E-01
8.00E+06,-5.00E-01
9.00E+06,-5.00E-01
1.00E+07,-5.00E-01
```

The script for converting the .listing files to .csv in **Appendix A.3**.

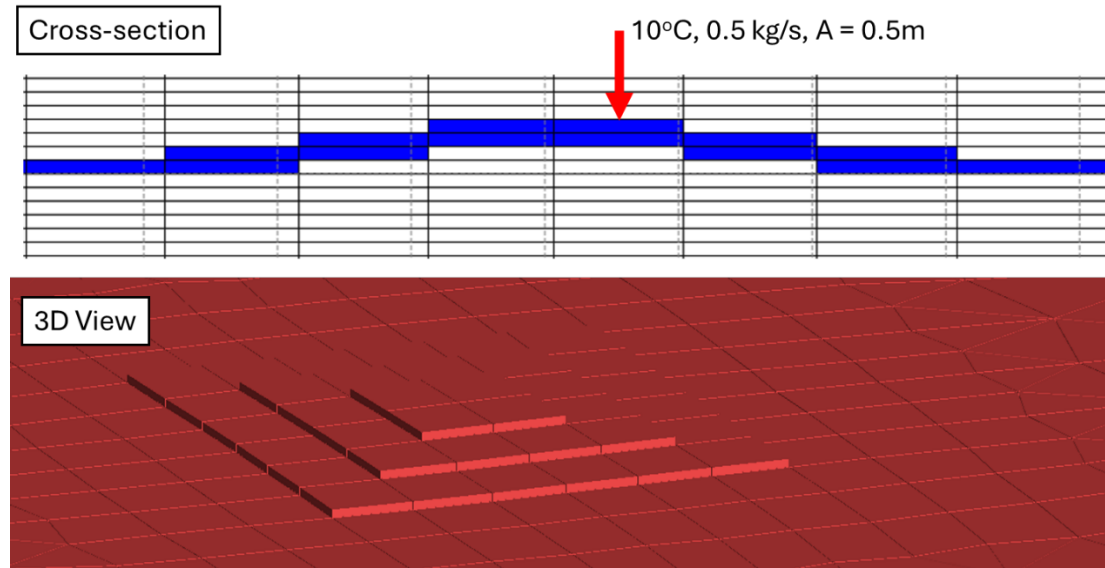
*analytical\_mts.py*

1. ###import required libraries###
2. import **numpy** as **np**
3. from **scipy.special** import **expi**
4. import **matplotlib.pyplot** as **plt**
5. import **pandas** as **pd**
- 6.
7. #Input the required parameters
8. **p0** = 3.47e+06 #Initial pressure in pa
9. **h** = 0.25 #thickness of aquifer in m
10. **k** = 5e-13 #Permeability in m-3
11. **v** = 1. e-6 #Fluid Viscosity
12. **r** = 1.12 #radius of the aquifer in m
13. porosity = 0.25
14. density = 1000
15. Crock = 1.e-10
16. Cfluid = 4.52e-10
17. compressability = Crock + Cfluid
18. **D** = (**k**/**v**)/(porosity\*density\*compressability) #Diffusivity in m2/s
- 19.

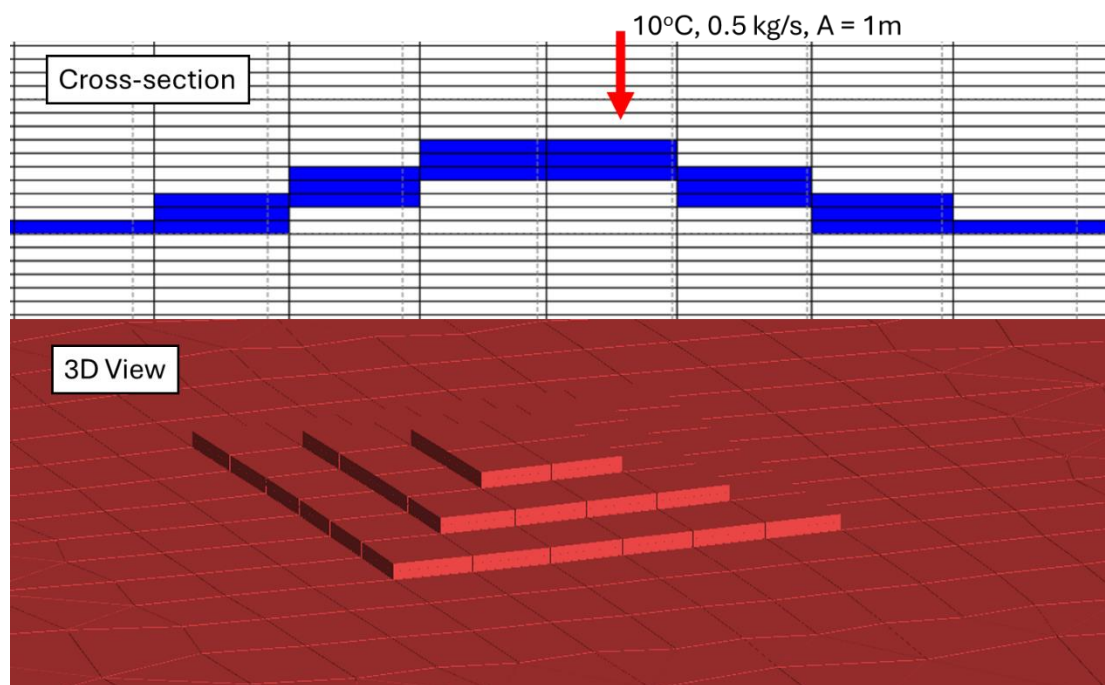
```
20. #time of transient in seconds
21. data = pd.read_csv('Flowrate.csv')
22. t = data['time'].values
23. qm = data['flowrate'].values
24. z = (r**2 / (4 * D * t))
25. #Pressure Calculations
26. p = p0 + (qm / (4 * np.pi * h * k / v)) * expi(z)
27. pbar = p/1e5
28.
29. #Script to Compare it with the numerical model solutions
30. press1 = np.loadtxt('04Radial.csv', delimiter=',')
31. press1_time = np.array(list(press1[:,0]))
32. press1_P = np.array(list(press1[:,1]))
33.
34. #Plot the graph!
35. plt.figure(figsize=(10, 5))
36. plt.xlabel('Time[bar]')
37. plt.ylabel('Pressure[bar]')
38. plt.title('Pressure vs Time')
39. plt.semilogx(press1_time, press1_P, color='red', label='Numerical')
40. plt.semilogx(t, pbar, color='blue', label='Analytical')
41. plt.grid(True)
42. plt.legend(loc='lower right')
43. plt.show()
```

## Appendix B.1 Wavy Model geometries

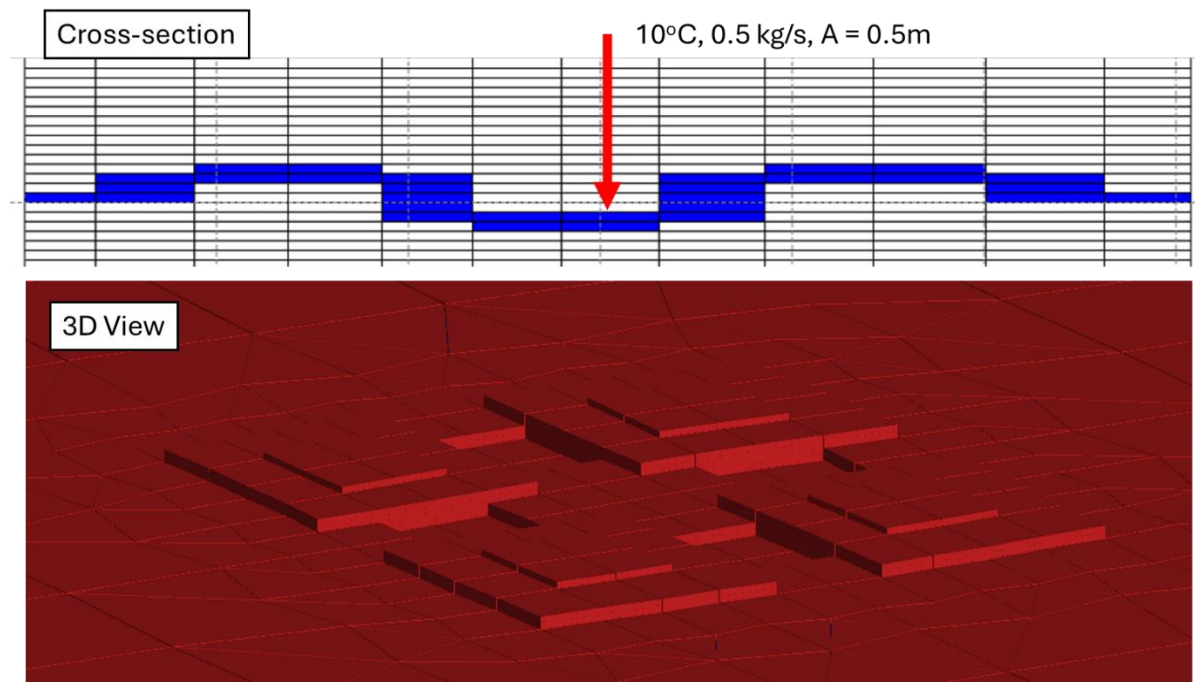
Case 1



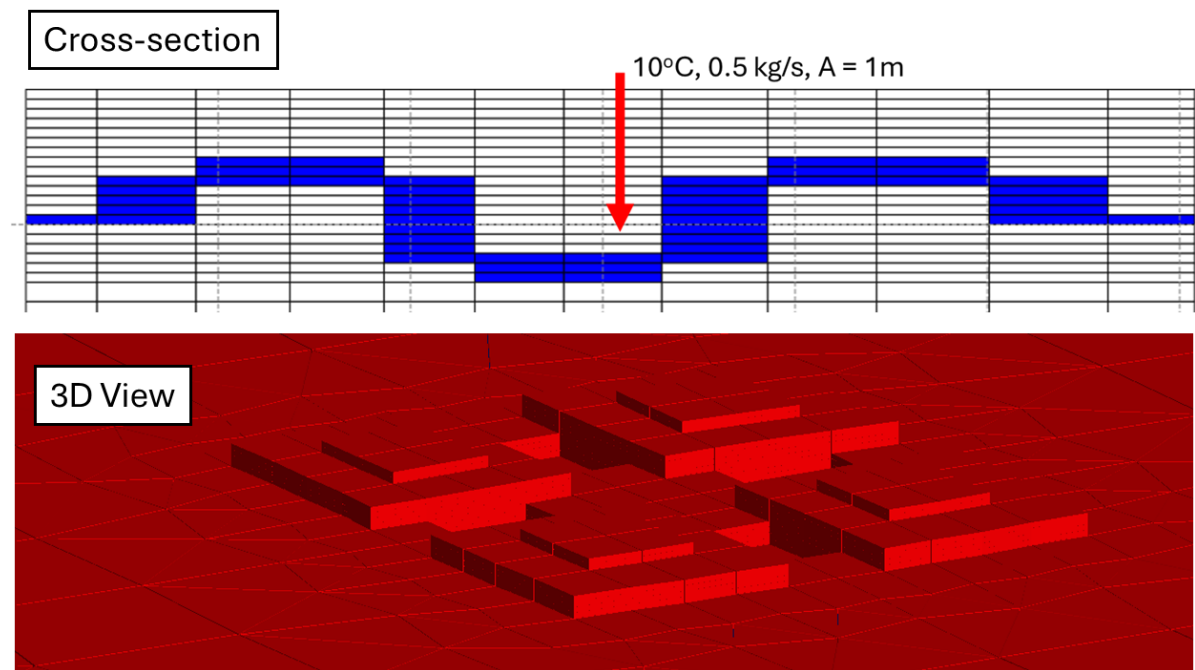
Case 2



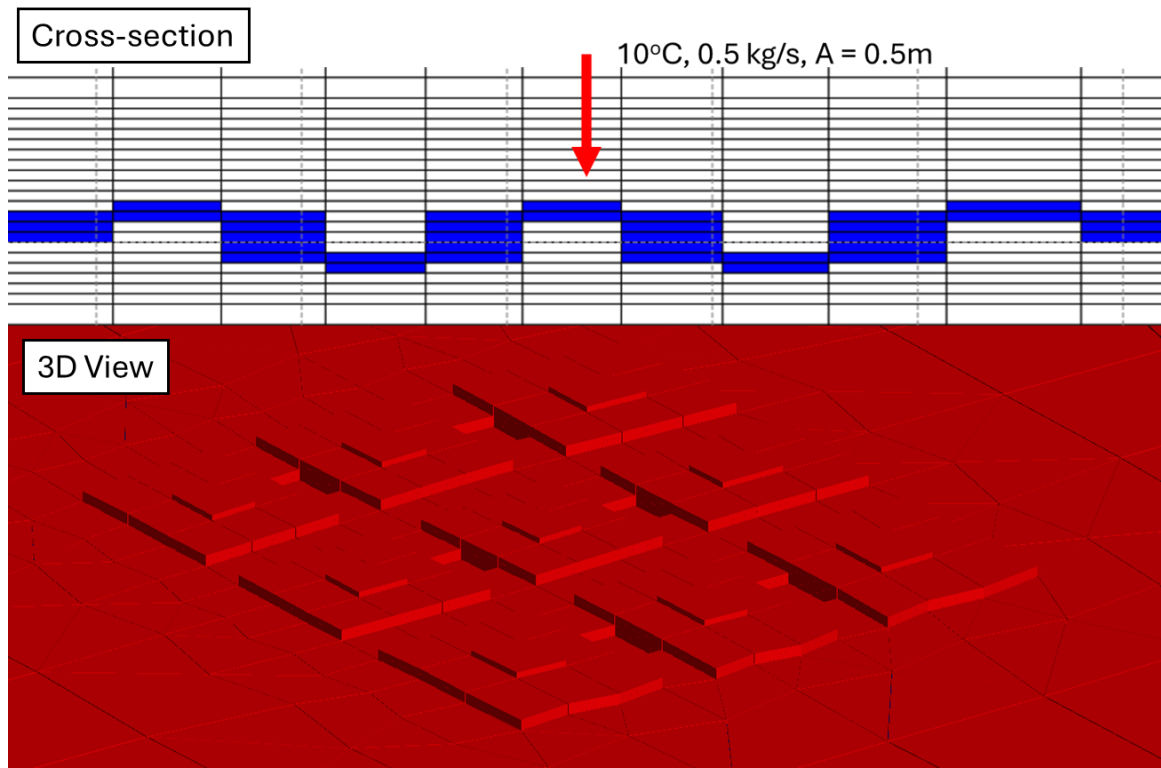
## Case 3



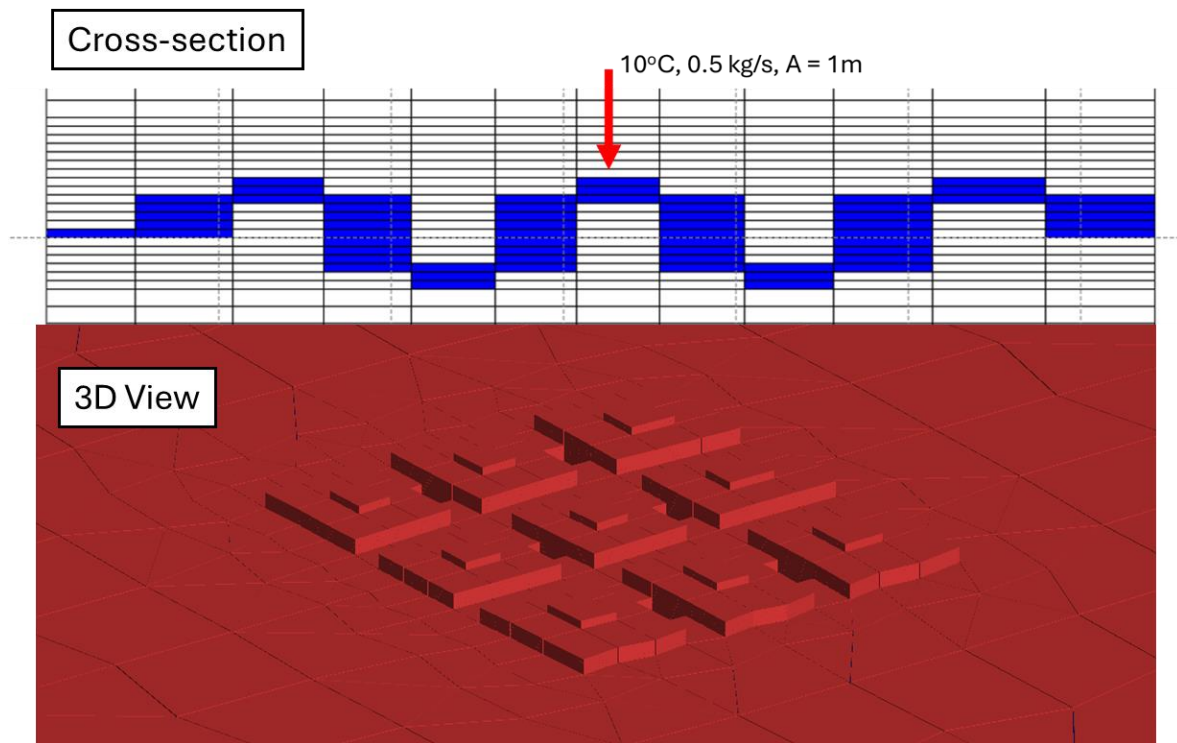
## Case 4



Case 5

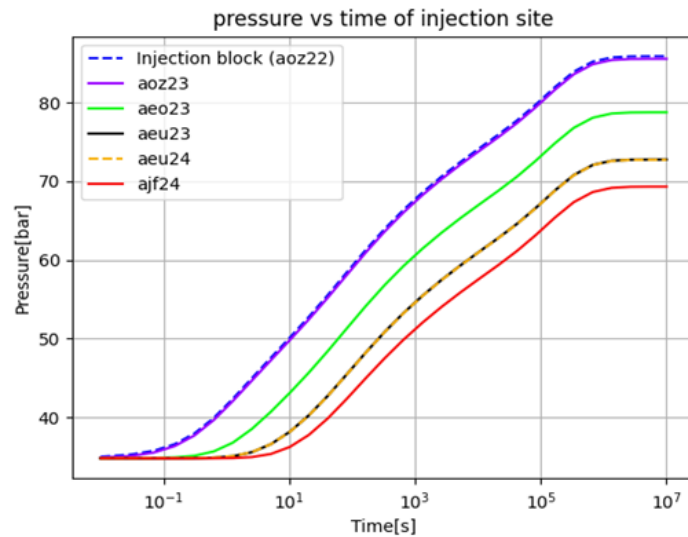


Case 6



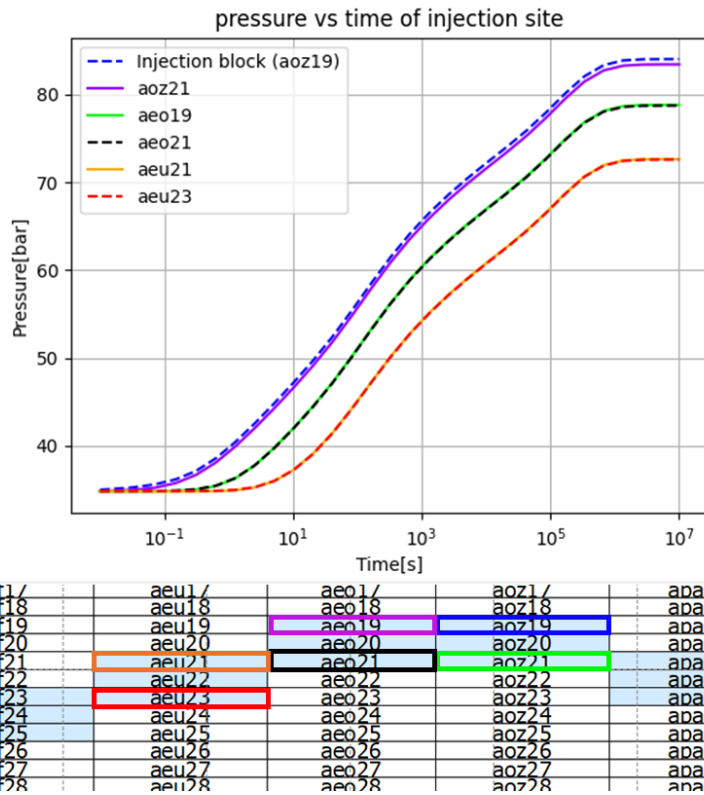
## **Appendix B.2. Pressure profile of selected block of wavy model**

Pressure profile at selected blocks which are chosen based on the mass flow direction of Case 1 shown below.

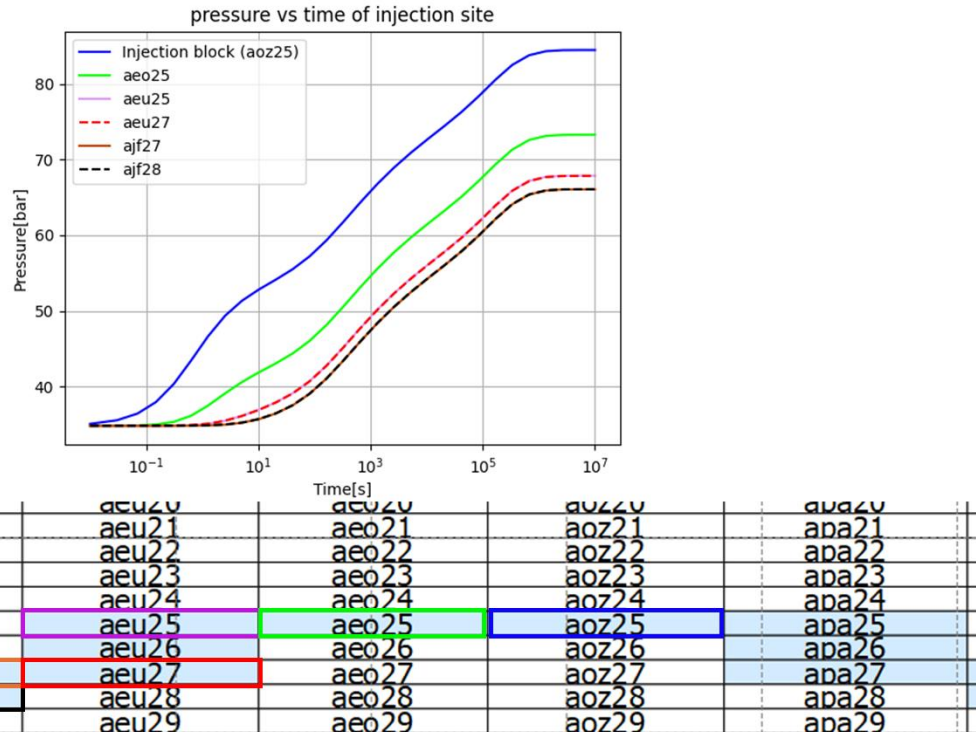


aif17	aeu17	aeo17	aoz17	apa17
aif18	aeu18	aeo18	aoz18	apa18
aif19	aeu19	aeo19	aoz19	apa19
aif20	aeu20	aeo20	aoz20	apa20
aif21	aeu21	aeo21	aoz21	apa21
aif22	aeu22	aeo22	aoz22	apa22
aif23	aeu23	aeo23	aoz23	apa23
aif24	aeu24	aeo24	aoz24	apa24
aif25	aeu25	aeo25	aoz25	apa25
aif26	aeu26	aeo26	aoz26	apa26
aif27	aeu27	aeo27	aoz27	apa27
aif28	aeu28	aeo28	aoz28	apa28
aif29	aeu29	aeo29	aoz29	apa29
aif30	aeu30	aeo30	aoz30	apa30

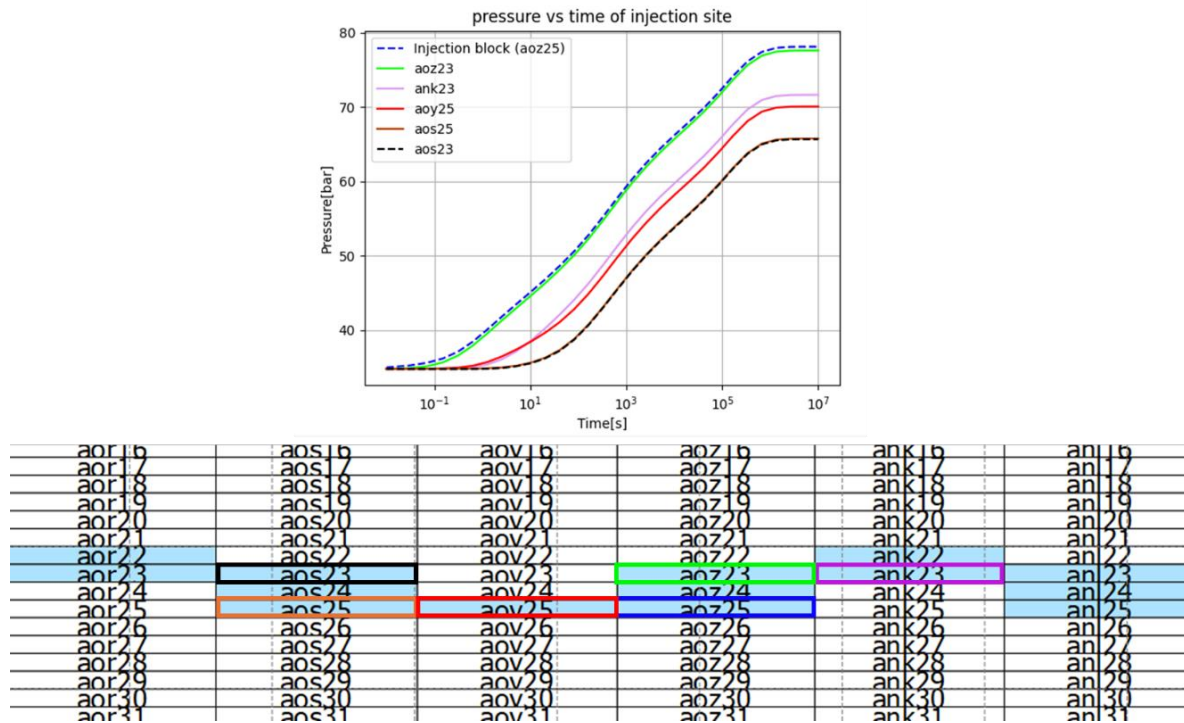
Pressure profile at selected blocks which are chosen based on the mass flow direction of Case 2 shown below.



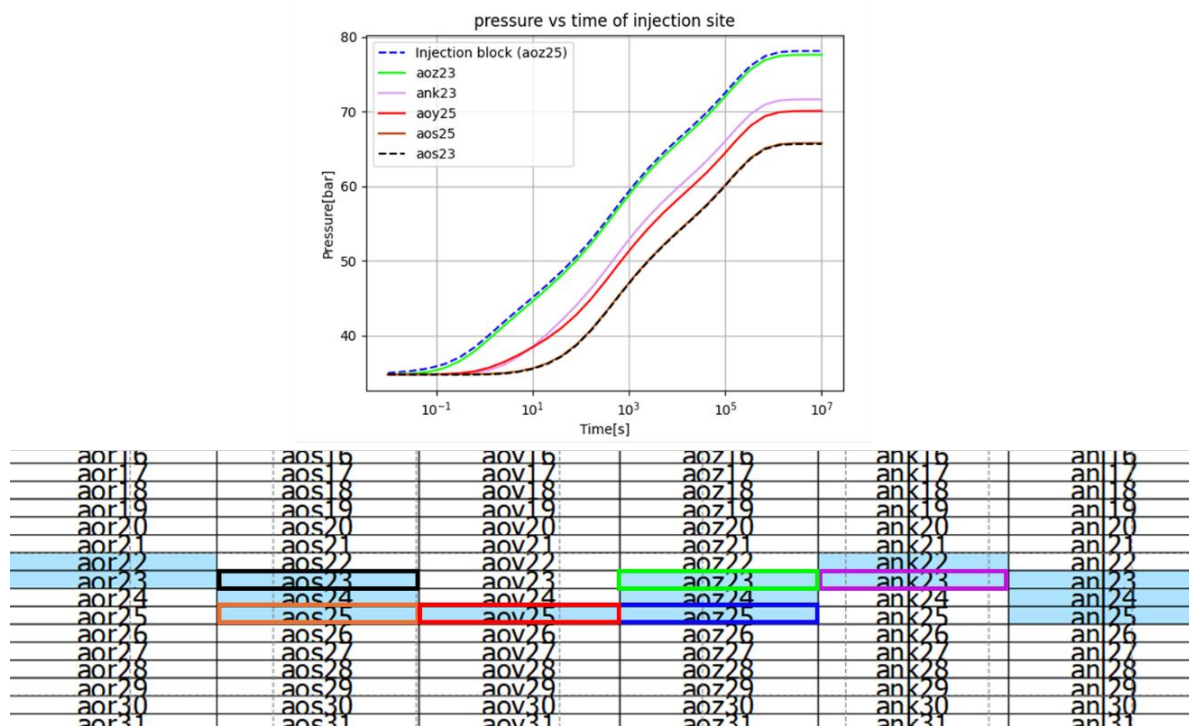
Pressure profile at selected blocks which are chosen based on the mass flow direction of Case 3 shown below.



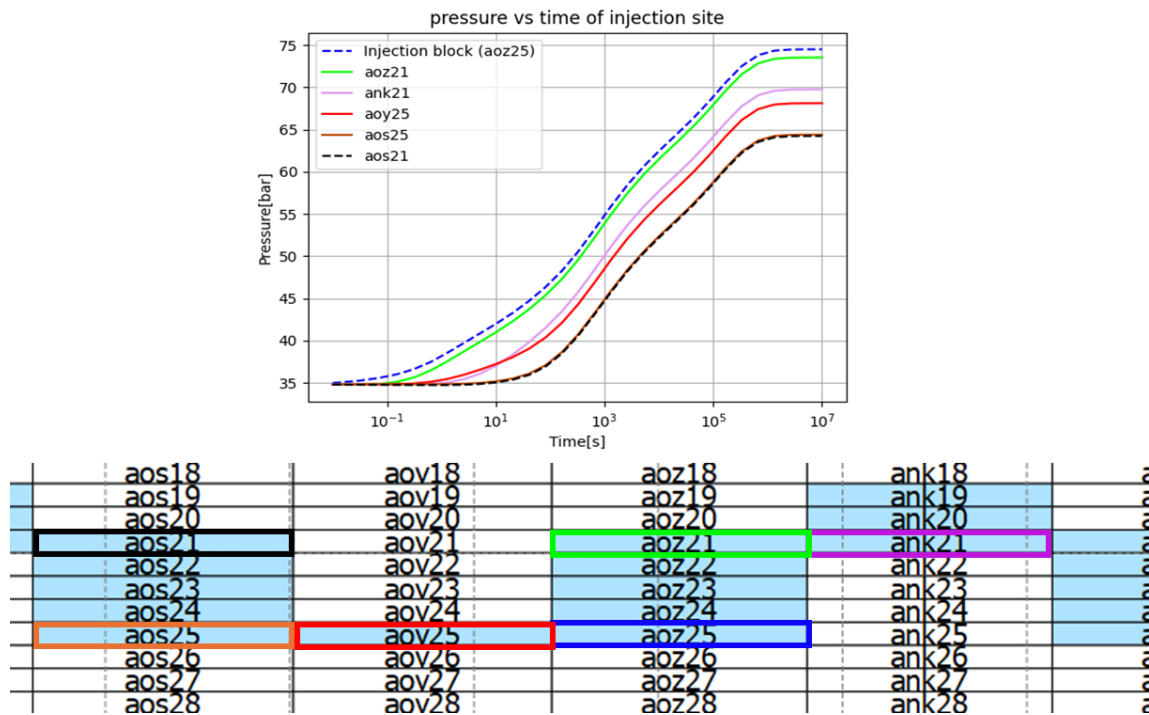
Pressure profile at selected blocks which are chosen based on the mass flow direction of Case 4 shown below.



Pressure profile at selected blocks which are chosen based on the mass flow direction of Case 5 shown below.



Pressure profile at selected blocks which are chosen based on the mass flow direction of Case 6 shown below.



# References

- Croucher, A. (2023). *PyTOUGH user's guide version 1.5.7*. Department of Engineering Science, University of Auckland.
- Fraedrich, W., & Heidari, N. (2019). *Iceland from the West to the South*. Springer Nature Switzerland.
- ISOR. (n.d.). *Jardfraedikort (Iceland Geology Map)* [Map].
- McLean, K. (2020). *Pressure Transient Analysis of Geothermal Wells: A Numerical Modelling Approach* [PhD Thesis]. University of Auckland.
- Newson, J. (n.d.). *Notebook: Constant Rate Test Results*.
- Nugraha, R. P., O'Sullivan, J., O'Sullivan, M., & Abdurachman, F. H. (2022). Geothermal Modelling: Industry Standard Practices. *Workshop on Geothermal Reservoir Engineering, 47th(SGP-TR-223)*, 12.
- O'Sullivan, M. (1987). Aspects of Geothermal Well Test Analysis in Fractured Reservoirs. *Transport in Porous Media, 2*, 497–517.
- O'Sullivan, M., Yeh, A., & Croucher, A. (2013). TIM - Yet Another Graphical Tool for TOUGH2. *35th New Zealand Geothermal Workshop, Rotorua, New Zealand*.
- Pruess, K., & Narasimhan, T. N. (1985). A Practical Method for Modeling Fluid and Heat Flow in Fractured Porous Media. *Society of Petroleum Engineers Journal, 25(1)*.
- Pruess, K., Oldenburg, C., & Moridis, G. (2012). *TOUGH2 User's Guide, Version 2*. U.S. Department of Energy.
- Sæmundsson, K., Sigurgeirsson, M. Á., & Friðleifsson, G. Ó. (2020). Geology and structure of the Reykjanes volcanic system, Iceland. *Journal of Volcanology and Geothermal Research, 391*, 106501. <https://doi.org/10.1016/j.jvolgeores.2018.11.022>

- Scott, S. W., Lévy, L., Covell, C., Franzson, H., Gibert, B., Valfells, Á., Newson, J., Frolova, J., & Guðjónsdóttir, M. S. (2022). *Valgarður: A Database of the Petrophysical, Mineralogical, and Chemical Properties of Icelandic Rocks* (1.2) [dataset]. Zenodo. <https://doi.org/10.5281/ZENODO.6980231>
- Theis, C. V. (1935). The relation between the lowering of the piezometric surface and the rate and duration of discharge of a well using groundwater storage. *Am. Geophys. Union Trans.*, 16, 519–524.
- Warren, J. E., & Root, P. J. (1963). The Behavior of Naturally Fractured Reservoir. *Society of Petroleum Engineers Journal*, 3, 245–255.
- Watton, T. J., Jerram, D. A., Thordarson, T., & Davies, R. J. (2013). Three-dimensional lithofacies variations in hyaloclastite deposits. *Journal of Volcanology and Geothermal Research*, 250, 19–33. <https://doi.org/10.1016/j.jvolgeores.2012.10.011>
- Widder, D. V. (1941). The Laplace Transform. *Princeton Mathematical Series*, 6 (Princeton University Press).
- Yeh, A., O’Sullivan, M., & Croucher, A. (2012). *Recent developments in the AUTOUGH2 simulator*.
- Zarrouk, S. J., & McLean, K. (2019a). Chapter 4—Introduction to pressure-transient analysis. In S. J. Zarrouk & K. McLean (Eds.), *Geothermal Well Test Analysis* (pp. 63–88). Academic Press. <https://doi.org/10.1016/B978-0-12-814946-1.00004-9>
- Zarrouk, S. J., & McLean, K. (2019b). Chapter 8—Numerical pressure-transient analysis modelling framework. In S. J. Zarrouk & K. McLean (Eds.), *Geothermal Well Test Analysis* (pp. 193–215). Academic Press. <https://doi.org/10.1016/B978-0-12-814946-1.00008-6>



